PREPARATION OF NANOEMULSION USING LIPASE-SYNTHESIZED GLUCOSE MONOOLEATE THROUGH LOW ENERGY TECHNIQUE

MUHAMMAD FAKHRURAZI BIN AHMAD FADZIL

FACULTY OF SCIENCE
UNIVERSITI MALAYA
KUALA LUMPUR

2021

PREPARATION OF NANOEMULSION USING LIPASE-SYNTHESIZED GLUCOSE MONOOLEATE THROUGH LOW ENERGY TECHNIQUE

MUHAMMAD FAKHRURAZI BIN AHMAD FADZIL

DISSERTATION SUBMITTED IN PARTIAL FULFILMENT OF THE REQUIREMENTS FOR THE DEGREE OF MASTER OF SCIENCE (BIOTECHNOLOGY)

INSTITUTE OF BIOLOGICAL SCIENCES
FACULTY OF SCIENCE
UNIVERSITI MALAYA
KUALA LUMPUR

2021

<div align="center">

UNIVERSITI MALAYA

ORIGINAL LITERARY WORK DECLARATION

</div>

Name of Candidate: **MUHAMMAD FAKHRURAZI BIN AHMAD FADZIL**

Matric No: **SOC 180011**

Name of Degree: **MASTER OF SCIENCE (BIOTECHNOLOGY)**

Title of Project Paper/Research Report/Dissertation/Thesis ("this Work"):

PREPARATION OF NANOEMULSION USING LIPASE-SYNTHESIZED GLUCOSE MONOOLEATE THROUGH LOW ENERGY TECHNIQUE

Field of Study: **NANOBIOTECHNOLOGY**

I do solemnly and sincerely declare that:

(1) I am the sole author/writer of this Work;

(2) This Work is original;

(3) Any use of any work in which copyright exists was done by way of fair dealing and for permitted purposes and any excerpt or extract from, or reference to or reproduction of any copyright work has been disclosed expressly and sufficiently and the title of the Work and its authorship have been acknowledged in this Work;

(4) I do not have any actual knowledge nor do I ought reasonably to know that the making of this work constitutes an infringement of any copyright work;

(5) I hereby assign all and every rights in the copyright to this Work to the University of Malaya ("UM"), who henceforth shall be owner of the copyright in this Work and that any reproduction or use in any form or by any means whatsoever is prohibited without the written consent of UM having been first had and obtained;

(6) I am fully aware that if in the course of making this Work I have infringed any copyright whether intentionally or otherwise, I may be subject to legal action or any other action as may be determined by UM.

Candidate's Signature   Date: 1st Mac 2021

Subscribed and solemnly declared before,

Witness's Signature   Date:

PREPARATION OF NANOEMULSION USING LIPASE-SYNTHESIZED GLUCOSE MONOOLEATE THROUGH LOW ENERGY TECHNIQUE

ABSTRACT

In this study, glucose monooleate (GluO) was synthesized and compared to its counterpart i.e. Tween-80 (Tw-80) and Span-80 (Sp-80) to investigate the influence of the different hydrophilic head structure of the surfactants on emulsification property. Utilizing sugar molecules like glucose as the hydrophilic head group of surfactants is of interest as it has a high potential to be used as a targeted delivery agent. The main objective of this study is to investigate the capability of lipase synthesized GluO in the formation of O/W nanoemulsion in four different types of vegetable oils that are sunflower oil, olive oil, palm oil, and coconut oil through low energy method. Initial screening showed that GluO as a single surfactant was not able to produce nanoemulsion. However, incorporation of Cremophor EL (CrEL) helped in the formation of oil-in-water (O/W) nanoemulsion in sunflower and coconut oil at optimal CrEL: GluO and S:O ratios of 63:37 and 60:40 respectively. The formation of O/W emulsion using GluO-incorporated surfactant mixture was studied using optical polarizing microscopy (OPM), small angle X-ray scattering (SAXS), and Fourier-transform infrared spectroscopy (FTIR). Based on the results, it is hypothesized that the mechanism of nanoemulsion production using GluO-incorporated surfactant mixture involved the formation of a bi-continuous/lamellar phase structure at 40 % water content rather than the formation of multiple emulsion (O/W/O) before it was dispersed into nano-sized oil droplets with further addition of water.

Keywords: sugar-fatty acid esters, glucose monooleate, nanoemulsion

PENYEDIAAN NANOEMULSI MENGGUNAKAN LIPASE-SINTESIS MONOOLET GLUKOSA MELALUI TEKNIK TENAGA RENDAH

ABSTRAK

Kajian ini adalah berkaitan dengan sifat pengemulsian Monoolet Glukosa (GluO) sebagai surfaktan yang menggunakan kepala hidrofilik yang berbeza daripada surfaktan Tween-80 (Tw-80) dan Span-80 (Sp-80). Menggunakan molekul gula seperti glukosa sebagai kumpulan hidrofilik berpotensi tinggi untuk digunakan sebagai agen penghantaran yang bersasar. Objektif utama kajian ini adalah untuk mengkaji kemampuan GluO dalam pembentukan nanoemulsi minyak dalam air (O/W) dalam empat jenis minyak sayuran iaitu minyak bunga matahari, minyak zaitun, minyak sawit dan minyak kelapa melalui kaedah tenaga rendah. Pemerhatian awal mendapati bahawa GluO tidak dapat menghasilkan nanoemulsi apabila digunakan secara tunggal. Walau bagaimanpun, penggabungan Kremofor EL (CrEL) membantu dalam pembentukan nanoemulsi O/W dalam minyak bunga matahari dan minyak kelapa pada nisbah Cr:EL: GluO dan S:O yang optimum iaitu masing-masing dari 63:37 dan 60:40. Mekanisma pembentukan nanoemulsi O/W dengan campuran surfaktan Cr:EL dan GluO telah dikaji dengan menggunakan mikroskopi polarisasi optik (OPM), hamburan sinar-X sudut kecil (SAXS) dan spektroskopi inframerah transformasi Fourier (FTIR). Berdasarkan maklumat yang diperolehi, hipotesis mekanisma pembentukan nanoemulsi dengan campuran surfaktan berasaskan GluO dapat dikenal pasti iaitu, ianya melibatkan pembentukan struktur fasa dwi-berterusan lamelar pada titik penyongsangan emulsi di kandungan air 40 % sebelum ianya tersebar ke titisan minyak bersaiz nano dengan penambahan air.

Kata kunci: ester gula, monoolet glukosa, emulsi-nano

ACKNOWLEDGEMENTS

In the name of the Almighty the Most Gracious and Most Merciful. Peace and blessings be upon Prophet Muhammad Saw.

Alhamdulillah, first and foremost to His Most Gracious and Merciful for bestowing me with many opportunities in this life to carry on.

I would like to express my deepest sense of gratitude to my supervisors, Professor Dr. Mohamad Suffian bin Mohammad Annuar and Dr. Khairul Anwar bin Ishak for the guidance, encouragement, remarkable knowledge, all the technical helps and advices throughout the entire project. I've gained precious experience and knowledge that prepared me for my next endeavor. Joining the Bioprocess and Enzyme Technology Lab has been a source of inspiration for me as it introduces me to a new set of environment and networks that opened an opportunity for collaboration work later on.

Finally, I wish to express my sincere thanks to my parents; Hj. Ahmad Fadzil Mohamad and Hjh Zaiton binti Mohd Shah and to my supportive wife, Mrs Noor Dina Wahid. Their affections and psychological support given me strength to complete the project. Without them, it would have not been possible for me to finish this journey. Finally, I dedicate my dissertation work to my childrens; Zara Delisha, Zara Sofea and Umar. May this be an inspiration for them to pursue knowledge and be a better person than I am.

Thanks also to all that have assisted me directly or indirectly throughout my master study. May Allah bless us all.

TABLE OF CONTENTS

LIST OF FIGURES

LIST OF TABLES

LIST OF SYMBOLS AND ABBREVIATIONS

CrEL : Cremophor EL

EIP : Emulsion inversion point

FTIR : Fourier-transform infrared spectroscopy

GluO : Glucose monooleate

NMR : Nuclear magnetic resonance

OPM : Optical polarizing microscopy

O/W : Oil in water

O/W/O : Oil in water in oil

PIC : Phase inversion composition

SAXS : Small angle X-ray scattering

SFAEs : Sugar-fatty acid esters

S:O : Surfactant to oil

S/O/W : Surfactant-oil-water

Sp-80 : Span-80

Tw-80 : Tween-80

W/O : Water in oil

W/O/W : Water in oil in water

LIST OF APPENDICES

CHAPTER 1: INTRODUCTION

An emulsion is a mixture of two immiscible liquid in which one phase dispersed in a droplet form (either micro- or nano-size) within the continuous phase (Perazzo et al., 2015; Singh et al., 2017). Nanoemulsions with a size range of 20 – 200 nm are of interest due to better adsorption and penetration property as well as kinetically stable as compared to microemulsion (Jintapattanakit, 2018; Perazzo et al., 2015; Zhang et al., 2011). Thus, it has the advantage to be used in various dosage forms such as creams, gels, an injectable and parenteral solution to deliver poor water-soluble or unstable pharmaceutical active ingredient (Ishak & Annuar, 2016; Singh et al., 2017). The emulsion system can exist in the form of binary phases such as oil-in-water (O/W) and water-in-oil (W/O) as well as multiple-phase (W/O/W and O/W/O) (Singh et al., 2017). For the drug delivery application, oil-in-water (O/W) emulsion system is preferred; as most bioactive compounds are lipophilic which are difficult to disperse in an aqueous medium without the proper encapsulation system (Ishak & Annuar, 2016; Ishak et al., 2017).

An emulsion can be prepared either through low energy, high energy or combination of both methods (Gupta et al., 2017; Gurpreet & Singh, 2018; McClements & Jafari, 2018). High energy methods use mechanical devices such as homogenizer or fluidizer to create shear force that breakdown the oil into smaller droplets (Gurpreet & Singh, 2018) while low energy methods rely on the surfactant self-assembly behaviour through composition, temperature and pH modulation of the emulsion system (Gurpreet & Singh, 2018; Ishak et al., 2017; McClements & Jafari, 2018).

The amphiphilic property of the surfactant plays an essential role in the formation and stabilization of an emulsion system. The basic structure of a surfactant consists of a hydrophilic head with various types (i.e., anionic, cationic or non-ionic) that is attached

to the hydrophobic tail as shown in Figure 1.1. The chemical structure of both parts (head and tail) can be modified to obtain different surfactant properties (Gu et al., 2013).
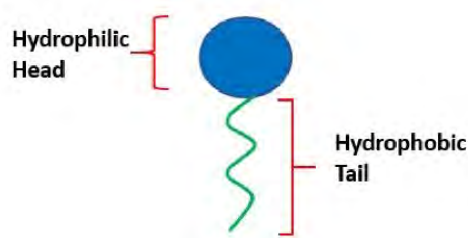
Figure 1.1: General structure of a surfactant.

In this study, we synthesized glucose monooleate (GluO) using lipase as the biocatalyst. This surfactant was compared to its counterpart i.e Tween-80 (ethoxylated sorbitan esters) and Span-80 (sorbitan esters) to investigate the influence of different hydrophilic head structure on the surfactant self-assembly behaviour. These three surfactants share a similar chemical structure of hydrophobic tail but different hydrophilic head structure. Surfactant with glucose as a hydrophilic head has high potential to be used in the encapsulation industry. Glucose is known to have a low level of toxicity and categorized as generally recognized as safe (GRAS) substance, high compatibility with components in foods and pharmaceuticals products. Also, it can be modified and functionalized with ligands to further conjugate with other molecules such as peptides, drugs, and oligonucleotides that can serve as a targeted delivery agent to treat infection and inflammation as well as for tumour diagnosis (Almuhaideb et al., 2011; Engelbrekt et al., 2009; Maratou et al., 2007).

To the best of our knowledge, the phase behaviour of the water-oil-surfactant system involving glucose monooleate (GluO) to produce nanoemulsion via low energy technique has never been studied. Therefore, the objectives of this research are:

i. To synthesize glucose monooleate (GluO) through enzymatic esterification of glucose and oleic acid.

ii. To study the formation of O/W nanoemulsion through phase inversion composition (PIC) using four different types of vegetable oils i.e. sunflower, olive, palm and coconut oil

CHAPTER 2: LITERATURE REVIEW

2.1   Properties of nanoemulsion

The terminology for conventional emulsion and nanoemulsion varies across literature with different mean size definitions (Jintapattanakit, 2018; Perazzo et al., 2015; Singh et al., 2017). In general, the emulsification system is a thermodynamically unstable system where phase separation will occur after a specific time (Gupta et al., 2016; McClements & Jafari, 2018; Singh et al., 2017). However, nanoemulsion is kinetically stable over conventional emulsion (Gupta et al., 2016) and exhibit smaller droplets size range (McClements & Jafari, 2018; Singh et al., 2017) which in turn make it less sensitive to physical and chemical changes (Gupta et al., 2016). The distinct difference of physicochemical properties of nanoemulsion over conventional emulsion is physical appearance, droplet size, and charge, rheology, and stability of the system (McClements & Jafari, 2018; Z. Zhang & McClements, 2018).

2.1.1   Physical appearance

The interaction of the light wave with the nanoparticles within the emulsification system gave a clear distinct property between nanoemulsion and conventional emulsion. Nanoemulsion is generally transparent as compared to the cloudy appearance of the conventional emulsion as a result of weak light scattering exhibit by the droplets size dimension relative to the wavelength of light (Jintapattanakit, 2018, Zhang & McClements, 2018). Theoretically, when emulsion particle size is larger than the wavelength of light, the light is scattered in all directions through reflection and

refraction, thus resulting in white and cloudy appearances of the solution. On the other hand, when the size of emulsion droplets is small in diameter than the wavelength of light, the light can pass through the dispersion resulting in translucent and transparent solutions (Chung & McClements, 2018; Zhang & McClements, 2018). Besides that, the concentration of droplets within the system may also influence the degree of lightness of the emulsion system in which higher concentration results in increasing lightness (McClements & Jafari, 2018). Droplet concentration is the volume of droplets per unit volume of nanoemulsion. The volume of droplets in the nanoemulsion system tends to be higher than conventional emulsion, which relates to the transparent and translucent characteristics of nanoemulsion (Jintapattanakit, 2018, Zhang & McClements, 2018). Other than that, the light scattering may also be affected by the refractive index of the droplets and the presence of chromophore within the emulsification system which will give the different colour appearances (Zhang & McClements, 2018).

2.1.2   Droplet size and charge

Droplet size is a crucial factor of an emulsion system that determines its stability against phase separation (Perazzo et al., 2015). As mentioned earlier, nanoemulsion consist of smaller droplet size tends to be more kinetically stable over a specific time compared to the conventional emulsion. Nanoemulsion system may have a wide distribution of droplet size range, and the simplest way to define the size is through particle size distribution (PSD) (McClements & Jafari, 2018; Zhang & McClements, 2018). The PSD will show the highest concentration of certain droplet size at the centre of the distribution curve and represent the average value of the droplet size of the system.

5

The most common formalism to describe the droplet size is droplet surface diameter, d_s or d_{32} (McClements & Jafari, 2018). The droplet size distribution directly depends on the emulsion formation either through high energy or low energy method which also influenced by other factors such as temperature, water addition rate, types of emulsifiers and ratio of surfactant to oil (Zhang & McClements, 2018).

The droplet charge of nanoemulsion depends on the types of surfactants and ionic composition of the solution within the system (Zhang & McClements, 2018). Generally, surfactants are divided into three main categories that are anionic, cationic, and non-ionic surfactants (Gu et al., 2013). Each of the surfactants possesses a different electric potential that may vary from positive, neutral and negative (Zhang & McClements, 2018). The surface charge of a droplet in nanoemulsion can be measured by zeta potential and the change in value may indicate the strength of repulsive or attractive forces among droplets that will eventually predict the stability of the nanoemulsion system (Gurpreet & Singh, 2018; Rodrigues et al., 2018).

2.1.3   Rheology

Rheology is another crucial aspect of nanoemulsion property that describes the overall flow pattern of the system (Gupta et al., 2016; McClements & Jafari, 2018; Zhang & McClements, 2018). Generally, nanoemulsion exhibits higher elasticity properties compared to macroemulsion (Gupta et al., 2016), and this comes with the agreement in having higher droplets concentration will give rise to the higher viscosity of the system (McClements & Jafari, 2018). Rheological properties of nanoemulsion

can be tuned to suit specific needs and applications. Robust and attractive interaction between droplets that will result in three-dimensional gel-like network formation within the system can be achieved by varying the salinity of the solution, pH, surfactant concentration and adding co-surfactants (Gupta et al., 2016). Understanding rheological properties of nanoemulsion may assist in the formulation of nanoemulsion formation, predict the stability of the system and determine the sensory attributes of final products such as thickness, creaminess and flowability (Zhang & McClements, 2018).

2.1.4   Stability

Nanoemulsion can be regarded as kinetically stable, but after some time, the system would eventually be destabilized. However, the time taken for this process to occur is more prolonged than conventional emulsion (Gupta et al., 2016; Gurpreet & Singh, 2018; McClements & Jafari, 2018; Singh et al., 2017; Zhang & McClements, 2018). Destabilization of the system can also be enhanced by the presence of various physical and chemical reactions such as oxidation, high temperature, and hydrolysis particularly for biodegradable nanoemulsion systems (Zhang & McClements, 2018). The destabilization mechanism includes flocculation, coalescence, Ostwald ripening and creaming or sedimentation as shown in Figure 2.1 (Gupta et al., 2016; Zhang & McClements, 2018).
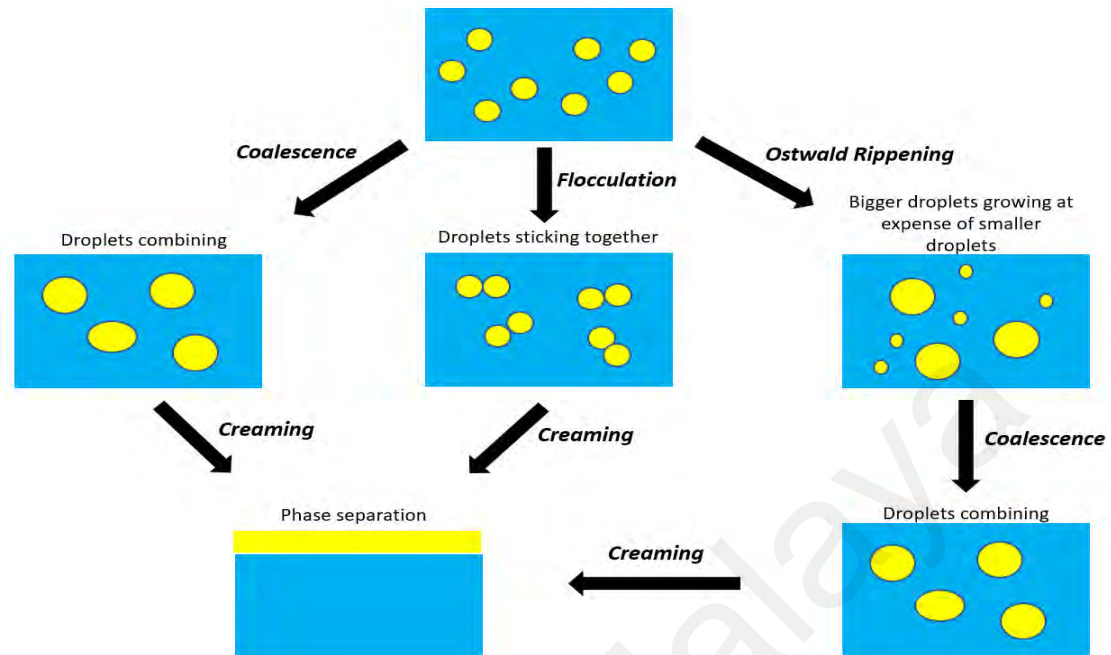
Figure 2.1: Destabilization mechanism of nanoemulsion system. Image adapted from Zhang & McClements, 2018.

Flocculation occurs when the droplets come close together without merging (Gupta et al., 2016). However, if the attraction force between droplets overcome the repulsive force and the droplets merge forming a single entity that exhibits larger droplets size, the process is known as coalescence (Gupta et al., 2016; Zhang & McClements, 2018). Meanwhile, Ostwald ripening is the result of differences in chemical potential of solute within droplets with different size distribution which will drive mass transfer from smaller droplets to larger droplets that will lead to growth of larger droplets and vice versa (Gupta et al., 2016; McClements & Jafari, 2018; Zhang & McClements, 2018). Creaming and sedimentation are the final destabilization mechanism that occurs as a result of flocculation and coalescence of the droplets (Gupta et al., 2016) because of gravitational force and phase density difference.

Creaming is a result of the lower density droplets than the surrounding system while sedimentation is a result of higher density properties of the droplets (Zhang & McClements, 2018).

2.2   Types of nanoemulsion

Nanoemulsion can be in the form of biphasic phase or simple emulsions such as oil-in-water (O/W) or water-in-oil (W/O) or multiple phases such as water-in-oil-in-water (W/O/W) and oil-in-water-in-oil (O/W/O) (McClements & Jafari, 2018; Singh et al., 2017). The formation of O/W or W/O nanoemulsion can be controlled by several factors such as properties of surfactants, method of emulsification (either top-down or bottom-up approach) and water content present in the system (Perazzo et al., 2015; Singh et al., 2017). Multiple phase nanoemulsion is not widely used and the method of preparing this type of nanoemulsion is complicated. Usually, multiple phase nanoemulsion is prepared by two-step approach in which it requires the formation of biphasic phase of nanoemulsion first (either O/W or W/O nanoemulsion) before it can be transformed in multiple phases with the aid of different surfactants which can be both lipophilic and hydrophilic type (McClements & Jafari, 2018; Singh et al., 2017). Therefore, the nature and types of surfactants used are critical in determining the types of nanoemulsion formation. For the application in drug delivery system, the oil-in-water (O/W) biphasic phase are of interest as most bioactive compound exhibit poor water solubility characteristics but showed high solubility in non-polar solvent (Ishak & Annuar, 2016; Ishak et al., 2017; Singh et al., 2017).

2.3 Oil phase in the emulsion system

The oil phase is an essential component of O/W nanoemulsion. A variety of oils can be used to formulate nanoemulsions such as free fatty acids, monoacylglycerols, diacylglycerols, triacylglycerols, flavour oils, essential oils, oil-soluble vitamins, and various lipophilic pharmaceutical compound. The formulation of food-grade nanoemulsion often used triacylglycerols such as sunflower oil, olive oil, palm oil, fish oil, soybean oil and coconut oil due to low cost, easily accessible and have an excellent functional attribute (McClements et al., 2017). However, the physicochemical characteristics of triacylglycerols such as having high interfacial tension and viscosity may pose challenges in the construction of nanoemulsion (Gurpreet & Singh, 2018). It is necessary to modify techniques and formulation to achieve nano-sized oil droplets when using these oils particularly medium and long-chain triacylglycerols (Gurpreet & Singh, 2018; Mcclements et al., 2017). In this literature review, several types of triacylglycerols such as sunflower oil, olive oil, palm oil and coconut oil will be discussed including their physicochemical properties as these food grade oils will be used in the construction of nanoemulsion.

2.3.1 Sunflower oil

Sunflower oil is a non-volatile vegetable oil that is extracted from sunflower seeds. The fatty acids composition of sunflower oil is made up of 90% unsaturated fatty acids primarily linoleic acid and oleic acid, and 8-9% of saturated fatty acids with palmitic acid and stearic acid as predominant fatty acids (Andhale & Kalbhor, 2018). Having a lower acid value (0.22 mg KOH/g) indicating low free fatty acids composition which

contributes to better oxidative stability compared to other types of vegetable oil (Andhale & Kalbhor, 2018; Arun et al., 2018). The iodine value of sunflower oil was found to be 147.23% which indicates that it contains more unsaturated fatty acids (Andhale & Kalbhor, 2018).

2.3.2 Olive oil

Olive oil can be obtained either through mechanical or chemical extraction of the fruit. Mechanical extraction is more preferred than chemical extraction as chemical extraction requires a refining process that may reduce the natural ingredients such as vitamins and polyphenols (Ashokkumar et al., 2018). Olive oil can be divided into different grades in which the one with the highest grade and quality is the extra virgin olive oil obtained by the cold press without any use of solvent. The fatty acids composition of olive oil differs depending on the extraction method, but in general, the predominant fatty acids are unsaturated fatty acids which made up to 83% of total oil content in which oleic acid is the most predominant type followed by linoleic acid and palmitoleic acid. The rest is stearic acid and linoleic acid which made up the saturated fatty acids composition (Ashokkumar et al., 2018). The iodine value of olive oil is lower than sunflower oil in which the value is 85.6% indicates a higher degree of saturation compared to sunflower oil (Andhale & Kalbhor, 2018; Ashokkumar et al., 2018).

2.3.3 Palm oil

Palm oil is derived from the fruits of the oil palm *Elaeis guineensis* (Akinola & Oguntibeju, 2010). Palm olein is one of the major palm oil products that domestically

and industrially used as cooking / frying oil. Palm olein is known to have high saturation content (Akinola & Oguntibeju, 2010; Boateng et al., 2016). The major components of palm oil are triacylglycerols (TAG) while monoacylglycerols (MAG) and diacylglycerols (DAG) are the minor components (Boateng et al., 2016). Unlike sunflower oil and olive oil, palm oil contains an equal mixture of high saturated (50.7%) and unsaturated fatty acids (49.3%) (Boateng et al., 2016; Mancini et al., 2015). Unsaturated fatty acids primarily come from oleic acid and linoleic acid, while major components of saturated fatty acids are palmitate and stearate (Mancini et al., 2015). The iodine value of palm oil is in the range of 47-50% indicates a higher level of saturation compared to sunflower oil and olive oil (Akinola & Oguntibeju, 2010).

2.3.4   Coconut oil

The application of coconut oil in various industries such as food, pharmaceutical, cosmetics, and nutraceuticals makes it an attractive candidate to be used as a carrier oil in nanoemulsion construction. Coconut oil is obtained from the mature kernel of the coconut (*Cocos nucifera L.*) (Aqilah et al., 2018). The methods to extract coconut oil from its kernel can be divided into a wet and dry method. The wet method does not involve heating or drying process but instead uses chilling and thawing, centrifugation, enzymatic and pH extraction method (Aqilah et al., 2018; Arumugam et al., 2014). The fatty acids composition of coconut oil consists of primarily saturated fatty acids (92%) while unsaturated fatty acids make up the rest of the fatty compositions (8%) (Arumugam et al., 2014). Saturated fatty acids composition primarily comes from lauric acid (47-50%), myristic acid (15-17%), capric acid (10%), caprylic acid (8%), palmitic

acid (7-8%) and stearic acid (2%) (Aqilah et al., 2018; Arumugam et al., 2014). The iodine value of coconut oil is the lowest (7.6%) compared to sunflower, olive and palm oil which reflects its high saturated fatty acids content (Arumugam et al., 2014).

2.4   Surfactants in the emulsion system

Several surfactants such as Tween-80, Span-80, Monoolein, Cremophor EL, etc. are frequently used as emulsifier to stabilize the dispersion of minute droplets of one liquid in another by lowering the surface tension between the two immiscible liquids; usually oil and water (Ishak & Annuar, 2016; Ishak et al., 2017; Kulkarni et al., 2011, Perazzo et al., 2015).

Based on their electrical charges, surfactants are divided into three types which are non-ionic, anionic, and cationic (McClements & Jafari, 2018; Zhang & McClements, 2018). In this study, we will be focusing on the non-ionic surfactants as it has broad compatibility in any solution as it does not carry any electrical charges and less sensitive to pH and ionic strength (McClements et al., 2017; Zhang & McClements, 2018). Besides that, non-ionic surfactants such as sorbitan esters (Tween and Span series) and sugar esters have been widely used in food and pharmaceutical industries due to their low toxicity and biodegradability in nature (McClements et al., 2017; Singh et al., 2017).

Both hydrophilic and hydrophobic group of surfactants plays an essential role in the reduction of surface tension in which will result in small droplets formation (Fuenmayor & Otoni, 2018; Perazzo et al., 2015). Hydrophilic lipophilic balance (HLB) is a concept that provides the value of an emulsifier affinity towards oil (HLB <10) or water (HLB

13

>10). HLB value will provide a basis for choosing a suitable surfactant to form either O/W or W/O nanoemulsion (Perazzo et al., 2015). In general, surfactants with high HLB value are suitable for the formation of O/W nanoemulsion (Fuenmayor & Otoni, 2018; Zheng et al., 2015).

2.4.1 Ethoxylated sorbitan esters (Tween surfactants)

This class of non-ionic surfactant is produced by the reaction of sorbitan fatty acid ester with ethylene oxide and is being commercially sold under the trade name "Tween". It is commonly used in the food and pharmaceutical industry as it has a high degree of compatibility with other chemicals and most importantly it is generally regarded as safe in terms of low toxicity and non-irritant materials (Mahdi et al., 2011; Mehta et al., 2010). Tween is a hydrophilic surfactant that tends to form oil-in-water emulsions. The HLB value of the Tween series ranges from 11 to 16.7 as shown in Table 2.1.

Table 2.1: Series of Tween surfactants.

Name	Hydrophobic Group	Types of Fatty Acids	HLB Value
Tween-20 (*polyoxyethylene sorbitan monolaurate*)	Laurate (C12)	Saturated	16.7
Tween-60 (*polyoxyethylene sorbitan monolaurate*)	Stearate (C18)	Saturated	14.9
Tween-80 (*polyoxyethylene sorbitan monooleate*)	Oleate (C18)	Unsaturated	15.0
Tween-85 (*polyoxyethylene glycol sorbitan trioleate*)	Oleate (C18)	Unsaturated	11.0

Figure 2.2 shows the molecular structure of different Tween series. The hydrophobic part of each series is different which results in different physicochemical properties and their ability to form nanoemulsion.
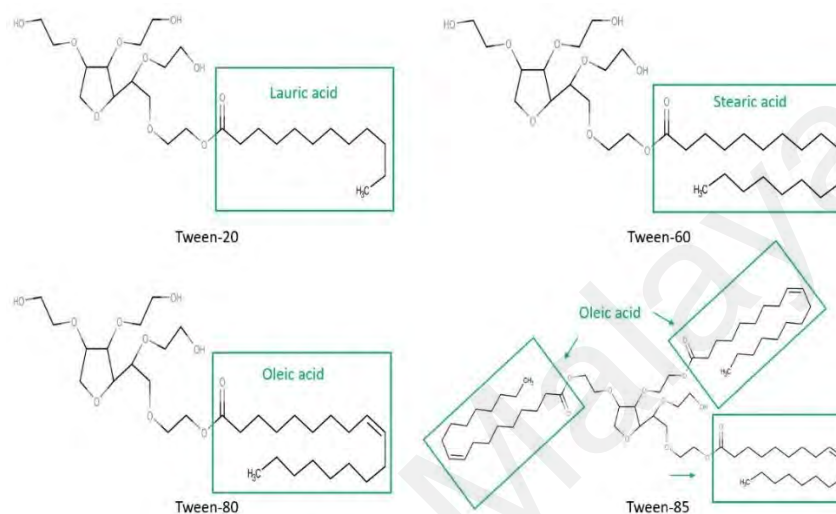
Figure 2.2: Chemical structure of Tween series.

2.4.2   Sorbitan esters (Span surfactants)

This class of non-ionic surfactant is made from sorbitol which is a sugar alcohol that is being esterified with fatty acids and exhibit the lipophilic property that makes it insoluble in water and tends to form a water-in-oil emulsion (Mahdi et al., 2011). As a derivative of Tween, Span is also commonly used as an ingredient to formulate pharmaceutical products or to be used as a vehicle in the food industry due to its low toxicity and non-irritant in nature (Mahdi et al., 2011; Mehta et al., 2010). However, the HLB value for Span series is low in value which ranges from 1.8 to 8.6 as shown in Table 2.2.

Table 2.2: Series of Span surfactants.

Name	Hydrophobic Group	Types of Fatty Acids	HLB Value
Span-20 (*sorbitan laurate*)	Laurate (C12)	Saturated	8.6
Span-60 (*sorbitan monooctacanoate*)	Stearate (C18)	Saturated	4.7
Span-80 (*sorbitan monooleate*)	Oleate (C18)	Unsaturated	4.3
Span-85 (*sorbitan trioleate*)	Oleate (C18)	Unsaturated	1.8

Figure 2.3 shows the molecular structure of different Span series. The difference in length of hydrophobic tail results in different properties among the Span series. Interestingly, with increasing carbon-chain length of the hydrophobic group, the entrapment efficiency increases (Khoee & Yaghoobian, 2017). which make one of the reasons why Span-80 is the most commonly used series in the construction of emulsion system (Dinarvand & Atyabi, 2005).
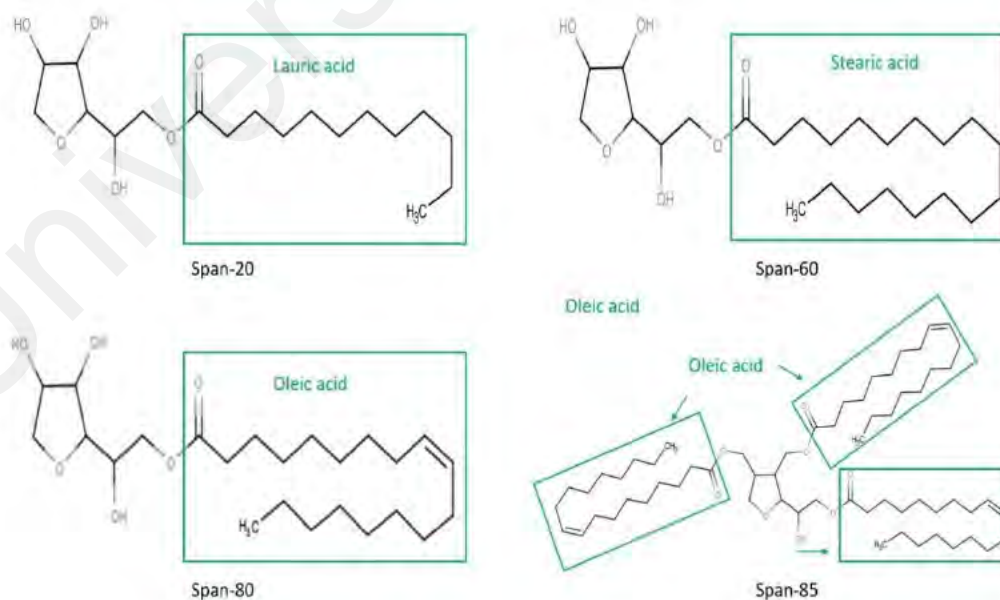
Figure 2.3: Chemical structure of Span series.

2.4.3   Polyoxyl 35 castor oil (Cremophor EL)

Cremophor EL (CrEL) is another type of non-ionic surfactant made by the reaction of castor oil with ethylene oxide and exhibits lipophilic properties with an HLB value ranges from 12 to 14.9 (Zeng et al., 2017). Structurally, about 35 moles of ethylene oxide are esterified to each molecule of castor oil (Figure 2.4). Cremophor EL (CrEL) is widely used in the pharmaceutical industry particularly serve as a vehicle for drug delivery of the lipophilic bioactive compound. It also is known to have good oil solubilization and encapsulation properties during emulsification process that often will result in small and fine oil droplets (Croy et al., 2017). Due to the low degree of ethoxylation compared to Cremophor 40, CrEL is better in solubilizing oil (Zeng et al., 2017) and will be used later in this study to formulate nanoemulsion using phase inversion composition technique.
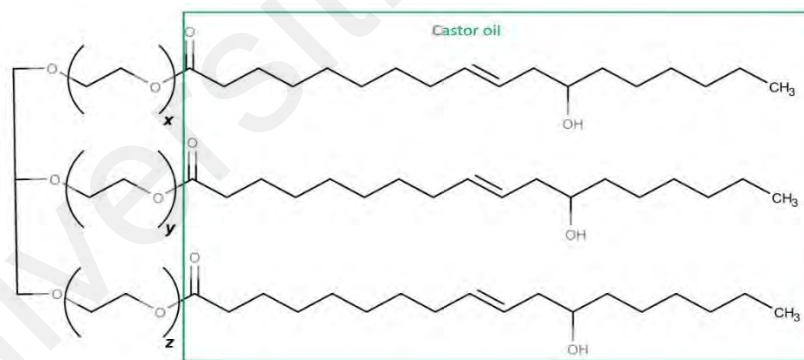
Figure 2.4: Chemical structure of Cremophor EL (x + y + z = 35).

2.4.4   Glycerol monooleate (monoolein)

Glycerol monooleate (also known as monoolein) is one example of commercially available surfactants that are commonly used in various industries such as pharmaceutical, cosmetics, and food industry (Kulkarni et al., 2011). As shown in

Figure 2.5, it consists of an oleic acid that is esterified to glycerol. The alkyl chain of the acid contributes to the hydrophobic tail while glycerol with two free hydroxyl groups provides the characteristic of the hydrophilic head. Due to the unsaturation in its alkyl chain, monoolein exists as an oily liquid at room temperature which has advantages to form smaller micelles in aqueous solution when compared to surfactants with saturated alkyl chains that exhibit solid form at room temperature (Bhadani et al., 2017).
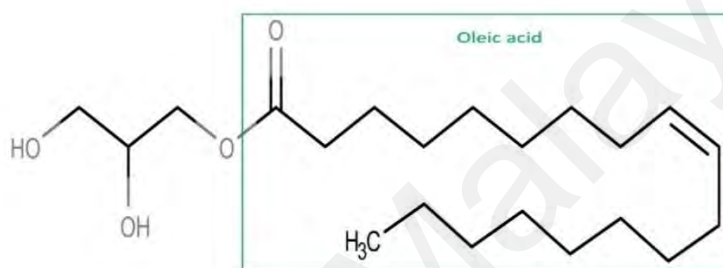
Figure 2.5: Chemical structure of Monoolein.

Monoolein is well known as a model lipid ester. The self-assembly behaviour of monoolein in ternary phase systems that consists of water, oil and surfactant has been widely studied (Kulkarni et al., 2011). Like other surfactants, monoolein will self-assemble at the interphase of water and oil (or nonpolar organic solvent). The phase behaviour of monoolein is remarkable as it can self-assemble into different liquid crystalline structures under varying conditions of temperature and solvent composition such as micelle (L_1), reverse micelle (L_2), lamellar ($L\alpha$), sponge-like structure (L_3), normal hexagonal (H_1), inverse hexagonal (H_2) and bi-continuous cubic phase (Kulkarni et al., 2011; Perazzo et al., 2015). Each shape and size of the phase structure have their distinct characteristics that may suit different applications (Kulkarni et al., 2011).

2.4.5   Sugar-fatty acid ester surfactants (SFAEs)

The increasing utilization of sugar-fatty acid esters (SFAEs) particularly in pharmaceutical and food industries is due its attributes of being non-toxic, biodegradable and highly compatible with bioactive compounds (Ahmad et al., 2012; Ariffin et al., 2014; Ishak et al., 2019; Klang et al., 2011; Mańko & Zdziennicka, 2015; Zhao et al., 2016). They are categorized as non-ionic surfactants (Ariffin et al., 2014) that exhibit amphiphilic property by having sugar molecule as hydrophilic head and alkyl chain as hydrophobic part. They may exist in waxy solid or oily liquid form depending on the types of fatty acids composition (Zheng et al., 2015). The most common saturated fatty acids used as alkyl donors are palmitic acids (C16) and stearic acids (C18) while unsaturated fatty acids are oleic acids (C18:1) and linoleic acids (C18:2) (Ariffin et al., 2014; Zheng et al., 2015). Unsaturated fatty acids with cis double bond tend to exist in oily liquid at room temperature compared to saturated fatty acids that may exist in solid form. Depending on the structure of their head-tail region, SFAEs have a wide range of HLB value (Zheng et al., 2015).

2.5   Advantages of using glucose-fatty acid ester in nanoparticle development

Glucose is a monomeric sugar molecule that is highly water-soluble, non-toxic, biodegradable and the primary energy source for most cells. Glucose transportation into cells occurs through two main mechanisms that are sodium-glucose linked transporters (SGLTs) and facilitated diffusion glucose transporters (GLUTs) (Navale & Paranjape, 2016). These glucose transporters are ubiquitously present in living cells especially monocyte, T & B lymphocyte, polymorphonuclear cell and natural killer cell during the

infection stage (Maratou et al., 2007). They are overexpressed especially during the activation or infection stage for high glucose uptake to activate the cells. Besides that, cancerous cells that are known for mass and rapid replication require more glucose than normal cells do as an energy source. Therefore, they change the expression of many genes in which one of them involves the overexpression of GLUT 1 transporter receptor for high glucose uptake (Wędrowski et al., 2018).

The overexpression of GLUT 1 transporters by these active cells provide the opportunity to make use of glucose for diagnosis purposes. For example, radioactive glucose or known as Fluorine-18 Fluorodeoxyglucose (FDG) can offer high sensitivity and specificity for diagnosis and restaging of solid tumour and metastatic cancer as compared to conventional imaging technology using CT scan and MRI (Almuhaideb et al., 2011). Other than that, the conjugation of glucose onto the gold-based nanoparticle shows potential benefits in which it can reduce the toxicity and increase the uptake of the nanoparticle by tumour cells (Engelbrekt et al., 2009). In addition, functionalized glucose that is attached to nanoparticle can be further conjugated with other molecules such as peptides, drugs, and oligonucleotides for targeted drug delivery application.

Besides commuting to the right destination (targeted delivery), a good delivery agent must have the ability to encapsulate the active compounds/drugs. By having these two properties, the delivery system may increase the drug's bioavailability. For this reason, we conduct a study to prepare an emulsion-based delivery system utilizing glucose monoleate (GluO) as the surfactant (Figure 2.6). The oil-swollen micelle of the emulsion can encapsulate lipophilic compounds within its oil core while the external glucose

contributes the advantages (as described before) to the nanoparticle. This GluO-stabilized emulsion system has good potential to be used for drug delivery in pharmaceutical applications.
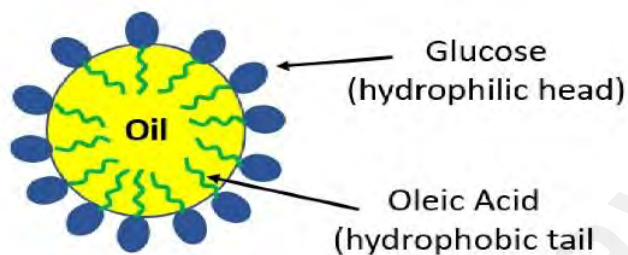
Figure 2.6: Oil-swollen micelle of O/W nanoemulsion.

2.6   Synthesis of sugar-fatty acid esters (SFAE)

Sugar-fatty acid esters can be synthesized through a chemical reaction that may form by-products and thus complicate the subsequent purification. Also, it is not an environmentally friendly approach that is in contrast with the green fingerprint of the sugar fatty acid esters (An & Ye, 2017; Zhao et al., 2016).

An enzymatic reaction that catalyzes the synthesis of SFAE is the greener alternative and a few studies have successfully conducted in this area. The application of immobilized enzymes such as Novozyme 435 and Lipozyme 435 in the synthesizing of SFAE was performed extensively with various findings. The lipase catalyzes the formation of an ester bond between acyl donor i.e. fatty acid and acyl acceptor i.e. sugar as shown in Figure 2.7 (Ariffin et al., 2014). The type of immobilized lipase used has different efficiency in SFAE formation which depends on the substrates. For example,

some lipases have a high selectivity for long- and medium-chain fatty acids than a shorter one (Gumel et al., 2011).
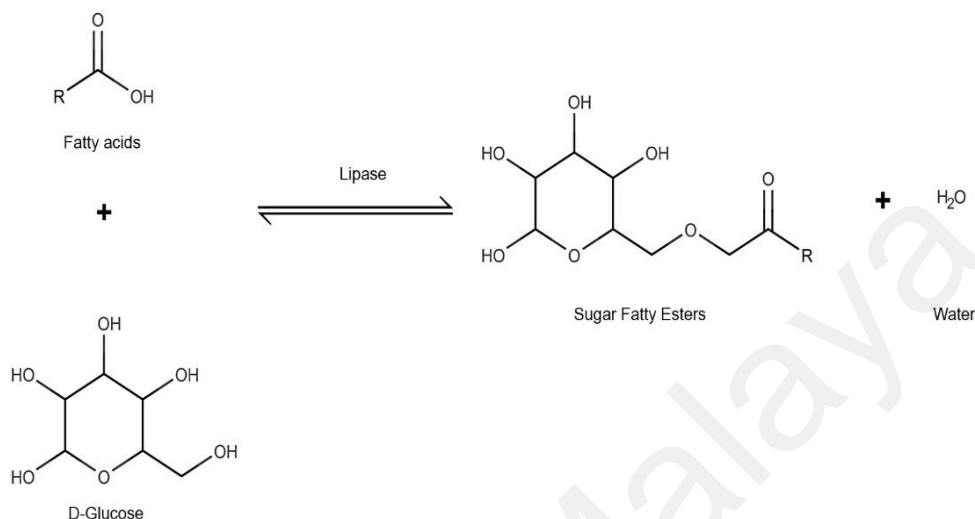
Figure 2.7: Lipase-catalyzed esterification of D-glucose with fatty acids.

Besides the enzyme, the solvent is also an important parameter to be considered in the production of SFAEs. Generally, an aqueous solvent is to be avoided, as it can affect the enzyme reaction that will lead to low product yield. However, in choosing non-aqueous solvent, one must consider the solubility and compatibility of substrates (sugar and fatty acids) towards the solvent (An & Ye, 2017; Ariffin et al., 2014; Zhao et al., 2016). A non-polar organic solvent is always preferred but sugar molecule showed poor solubility in these solvents and may reduce the reaction yield. A previous study showed successful esterification of methyl glucose and lauric acid by using an ionic liquid, consisting quaternary ammonium salt with a mixture of amine and amide, as the reaction solvent to solubilize both molecules along with immobilized lipase (Zhao et al., 2016). The ratio of alkyl donor (fatty acids) and alkyl acceptor (sugar) also play an important role in the esterification reaction. The solubility of a substrate in the reaction medium

may be affected by the concentration of the other substrate as the dissolution of a substrate affects the polarity of the reaction medium. A study performed the enzymatic esterification of capric acid as acyl donor and methylated glucose as acyl acceptor in a mol ratio of 3:1 with 2 gram of lipase enzyme per acyl acceptor in which give the best yield of SFAE formation (Ariffin et al., 2014). Other important factors in SFAE production are described in Table 2.3.

Table 2.3: Sugar-fatty acid ester production in various conditions.

Acyl Donor	Acyl Acceptor	Enzyme	Solvent	References
Decanoic acid	Methylated glucose	Lipase B	Tert-butanol	Ariffin et al., 2014
N-acyl amino acid	Methylated glucose	Lipozyme 435	Tert-butanol	An & Ye, 2017
Palmitic acid	Methylated glucose	Novozym 435	1-hexyl-3-methylimidazolium trifluoromethylsulfonate	Zhao et al., 2016
Vinyl laurate	D-glucose	Lipozyme TLIM	1-hexyl-3-methylimidazolium trifluoromethylsulfonate	
Palmitic acid	D-glucose	Lipase B	DMSO: tert-Amyl alcohol (80:20)	Ren & Lamsal, 2017
Lauric acid	D-glucose	Lipase B	DMSO: tert-Amyl alcohol (80:20)	
Hexanoic acid	D-glucose	Lipase B	DMSO: tert-Amyl alcohol (80:20)	

2.7 Formation of O/W nanoemulsion

Nanoemulsion can be produced through two main techniques that are high energy and low energy method. Although the name of method interchangeably different across literature such as top-down, bottom-up, phase inversion, persuasion, and Brute force method, the basic principle of the different method will fall either in one of the two broad category (Fuenmayor & Otoni, 2018; Gupta et al., 2016; Gurpreet & Singh, 2018; Roger, 2016; Singh et al., 2017).

2.7.1 High energy method

High energy method requires mechanical devices such as homogenizer, ultrasonicator, colloid mills and microfluidizer that provide the external mechanical energy to break down the bulk oil phase into smaller droplets (Singh et al., 2017). These mechanical devices provide pressure and stress onto the emulsion system in the form of shear, grinding, turbulence, attrition and high-frequency wave for breaking down the large oil drops (Gurpreet & Singh, 2018; Singh et al., 2017). However, one need to consider maintenance cost for the devices and high energy utilization despite faster nanoemulsions generation (Fuenmayor & Otoni, 2018; Roger, 2016). Also, high mechanical energy may cause a spike increase in temperature of emulsion solution which is the major drawback for encapsulating thermally sensitive active compounds or drugs (Håkansson & Rayner, 2018).

2.7.2 Low energy method

Low energy method or also known as bottom-up, phase inversion emulsification (PIE) or persuasion method involves in harvesting the free energy within the interactive system of water-oil-surfactant (W/O/S) upon the change in temperature, pH or composition (Fuenmayor & Otoni, 2018; Gurpreet & Singh, 2018; Ishak et al., 2017; Roger, 2016). No high mechanical energy generator of devices is needed to produce nanoemulsion *via* this approach, thus called a low energy method (Fuenmayor & Otoni, 2018; Gurpreet & Singh, 2018; Singh et al., 2017). Phase inversion is a method that involves the changes in surfactant orientation from curved towards water (W/O) to curved towards oil (O/W) or vice versa (Fuenmayor & Otoni, 2018; Gurpreet & Singh, 2018) that is triggered by changes in temperature or composition of the water-oil-surfactant system (W/O/S) (Figure 2.8).
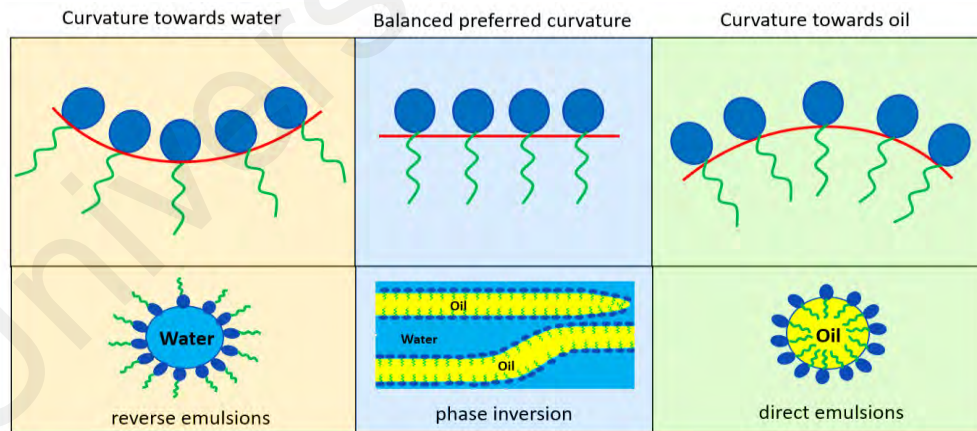
Figure 2.8: Different types of preferred curvature in the surfactant layer. Image adapted from Roger, 2016.

In phase inversion temperature (PIT), the system starts with a coarse emulsion of W/O in a specific temperature above the phase inversion temperature (PIT) of the surfactant mixture, and when the system is cooled down, the system passes through PIT which will then result in the surfactants shifting from W/O towards O/W and small droplets are formed (Fuenmayor & Otoni, 2018; Gupta et al., 2016).

Meanwhile, in phase inversion composition (PIC), the water-oil-surfactant system (W/O/S) is modulated to produce O/W nanoemulsion via gradual increment of changes in composition, particularly, water as illustrated in Figure 2.9. Technically, it starts with the formation of the reverse water-swollen micelle (W/O emulsion) towards the formation of solid lamellar/bi-continuous structure and eventually to normal oil-swollen micelle (O/W emulsion). Bi-continuous/lamellar structure is formed at the emulsion inversion point (EIP) and very important as it determines the final size of oil droplets in the emulsion solution. Without a proper formation of this structure, the non-polar oil cannot be gradually dispersed into nano-sized droplets (Ishak & Annuar, 2016; Ishak et al., 2017).
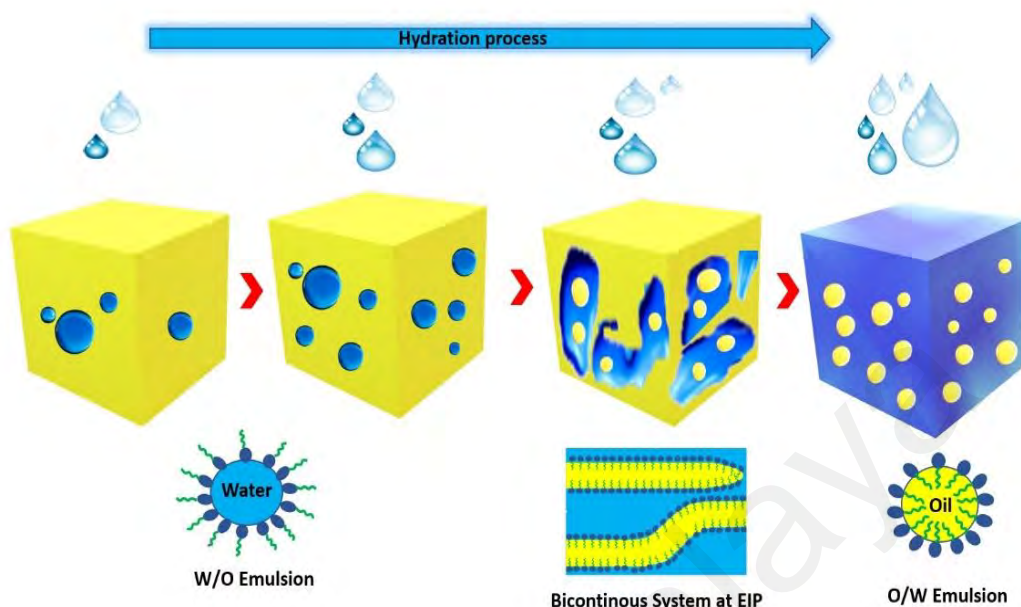
Figure 2.9: O/W nanoemulsion formation in PIC method. Image adapted from Perazzo et al., 2015.

2.8   Factors affecting O/W nanoemulsion formation through phase inversion composition (PIC)

The preparation of O/W nanoemulsion employing PIC method involves two main parts which are mixing the oil and surfactant (which is going to be the dispersed phase) and titration of aqueous solvent/medium (the continuous phase) into the oil-surfactant mixture with constant stirring. A few crucial factors were identified to give significant influence on the emulsification process such as the pH, viscosity, density of solvent/medium, stirring rate as well as water addition rate (Ishak et al., 2017; Perazzo et al., 2015; Roger, 2016). Some examples of nanoemulsion formation studies employing PIC method but with different processing conditions are shown in Table 2.4.

Besides the aforementioned parameters, the shape of surfactants also influences the formation of nanoemulsion through PIC (Perazzo et al., 2015; Roger, 2016). This is because it determines the phase behaviour and structure of the water-oil-surfactant system especially at EIP whereby surfactants would align in between oil and water phase stream to form a solid lamellar/bi-continuous structure as interfacial tension is minimized. Without a proper formation of the bi-continuous structure, a course liquid O/W emulsion instead of O/W nanoemulsion will be produced (Ishak & Annuar, 2016; Ishak et al., 2017). Therefore, an extensive study of phase behaviour and structure of a water-oil-surfactant system is important as it provides an understanding of physical and chemical aspects in the emulsification process (Kulkarni et al., 2011; Perazzo et al., 2015; Roger, 2016).

Table 2.4: Example of emulsification study employing PIC technique.

Oil Phase	Surfactant	Co-surfactant	Processing Condition	Droplet size (average)	References
Decane	Brij 30 (polyoxyethylated lauryl ether)	None	• Stirring rate 700 rpm • Water addition rate 0.5 ml/min • Concentration of surfactant at 5% wt	50 nm	Forgiarini et al., 2014
Miglyol 818 (*Caprylic/ Capric/ Succinic Triglyceride*)	Polisorbat 40	n-butanol	• Stirring rate 300 rpm • Slow titration of water • Concentration of surfactant at 23.5% wt • pH 7	115.9 nm	Jaworska et al., 2014

Mixture of jojoba oil and mcl-PHA	Cremophor EL	Span 80	• Intermittent vortexing
			• Slow titration of water
			• Concentration of surfactant at 2.5% wt,
			• Best optimum ratio :
			  ○ S/O = 70:30
			  ○ W/(S/O) = 86:14
			  ○ Cremo/Sp80 = 63:37
				< 50 nm	Ishak et al., 2017

Vegetable oil	Polyglycol polyricinoleate (PGPR)	Polyglycerol fatty acid ester (PGFA)	• Stirring rate 300 rpm • Glycerol in water added in one step to make final aqueous conc at 99% • Best optimum ratio : ○ S/O = 80:20	< 50nm	Wakisaka et al., 2015

2.9   Self-assembly and phase behaviour of surfactant in phase inversion composition (PIC)

Self-assembly characteristics of surfactants in aqueous solvent are the driving force in the formation of various supramolecular shape with different dimensions such as micelle (L_1), reverse micelle (L_2), lamellar ($L\alpha$), sponge-like structure (L_3), vesicles (L_4), normal hexagonal (H_1), inverse hexagonal (H_2) and bicontinuous cubic phase Kulkarni et al., 2011; Perazzo et al., 2015). The formation of micelles only happens above a specified concentration of surfactants which is known as critical micellar concentration (CMC) (Kulkarni et al., 2011; Perazzo et al., 2015).

Figure 2.10 shows the formulation-composition map that has been widely used as a reference for studying and preparing emulsion (Ishak & Annuar, 2016; Perazzo et al., 2015). It provides the physicochemical understanding of phase behaviour of water/oil/surfactant system during emulsification. The zigzag line refers to the inversion line of the surfactants; from W/O to O/W or vice versa with changes in oil-water composition. On the left side of the inversion line, are oil continuous (A^+, B^+ and B^-) while on the right side is water continuous (A^-, C^-, and C^+). The emulsions system located in A^-, A^+, B^+ and C^- are stable normal emulsion (O/W or W/O) while the systems located in B^- and C^+ are abnormal emulsion (W/O/W and O/W/O). Hydrophilic-lipophilic deviation (HLD) is a parameter that characterizes the behaviour of a surfactant in the emulsion system (Perazzo et al., 2015). For instance, HLD > 0 (at + region of the formulation-composition map in Figure 2.10), the surfactant has more affinity towards oil and the opposite occurs for HLD < 0. When HLD = 0, the surfactant has both affinities towards oil and water; hence, bi-continuous lamellar order can be formed

(Ishak & Annuar, 2016). The shaded line in the middle of the inversion line refers to the transitional inversion line. Theoretically, at the right formulation with a balanced amount of water and oil, the system can pass through the transitional inversion line in which a bi-continuous lamellar structure can be formed.
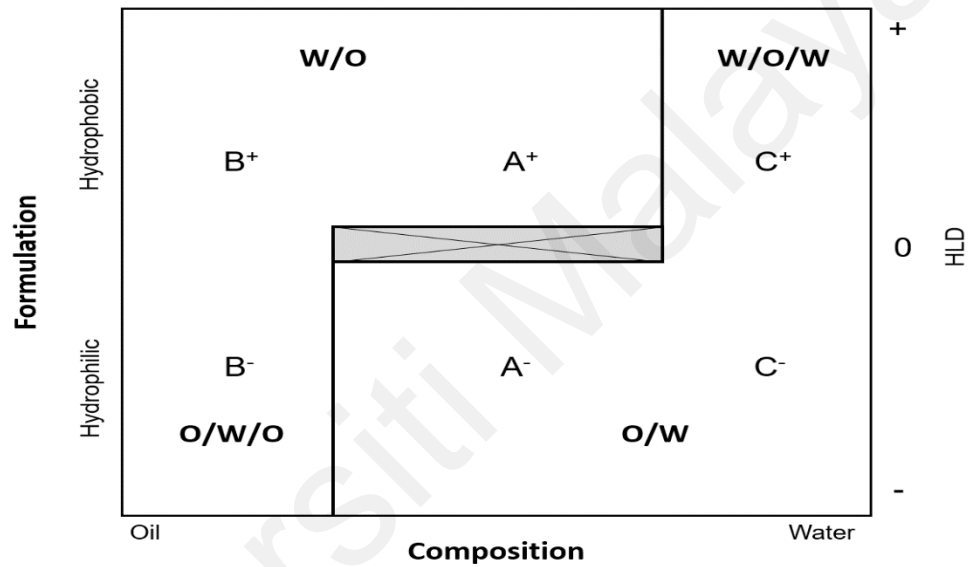
Figure 2.10: Formulation-composition map of emulsions system. The shaded line in the middle of the inversion line refers to the transitional inversion line.

2.10 Analysis of water-oil-surfactant phase system during emulsification

2.10.1 Optical polarizing microscopy (OPM)

Theoretically, the formation of nanoemulsion through the PIC method requires the formation of a bi-continuous structure or lamellar structure at emulsion inversion point (EIP) before it is dispersed into fine oil droplets with further addition of water (Perazzo et al., 2015; Roger, 2016). This bi-continuous structure formation indicates balanced intermolecular interaction among water, oil and surfactant and the structure which is anisotropic structure shows birefringence characteristics when cross-polarized with light using optical polarized microscopy (OPM). OPM is a simple and straightforward method to detect the presence of anisotropic structure in liquid crystals. The presence of birefringence during the preparation of nanoemulsions needs to be monitored to identify the formation of a bi-continuous structure as it will determine the final size of oil droplets in an emulsion solution. Without the proper formation of a bi-continuous lamellar structure at emulsion inversion emulsion point (EIP), the oil cannot be gradually dispersed into nano-sized droplets (Ishak & Annuar, 2016, 2017).

2.10.2 Small angle X-ray scattering (SAXS)

The characterization of the liquid crystal structure at EIP can be investigated through the interpretation of X-ray scattering patterns. Small-angle X-ray scattering (SAXS) plays an important role in providing supporting information on the shape and structure of nano-scale liquid crystals during the emulsification process (Li et al., 2016; Tyler et al., 2015). Therefore, SAXS provides detail information on a structure as compared to

the microscopy technique. Surfactants are well known to have spontaneous self-assembly characteristics into various liquid crystalline structures with various ranges of interaction among the structural order. Scattering patterns that appear in SAXS give information on the long-range orders of the structure hence the lattice parameter and types of structure can be determined (Tyler et al., 2015). Besides that, SAXS can give information up to angstrom or nanoscales level.

2.10.3   Fourier-transform infrared (FTIR)

Fourier-transform infrared (FTIR) spectroscopy is widely used to investigate the intermolecular interaction of the emulsions component by observing the changes in the functional group spectra of the surfactant-oil-water system. Previously, infrared spectroscopy was traditionally used to determine the critical micelle concentration of surfactants from the shift of the C-H bend (Devanathan et al., 1991). Considering the low energy method of the emulsification process, particularly employing the PIC technique, FTIR comes into handy by providing the spectral data of intermolecular interaction. PIC technique involves the dilution process of the surfactant-oil system with water hence, the changes in the functional group's spectra such as C-H and O-H band can be monitored (Lv et al., 2014). The spectral information can provide data on emulsion inversion point (EIP), phase transition of emulsion system and intensity of intermolecular interaction between molecules within the system thus give the idea on the mechanism of the emulsion formation (Lv et al., 2014).

CHAPTER 3: METHODOLOGY

3.1 Materials and Reagents

Synthesis of Glucose Monooleate (GluO): All materials and chemicals used were those from standard chemistry items except for D-glucose monohydrate (>99%) and oleic acid (>99%) was purchased from Sigma-Aldrich while immobilized enzyme of *Candida antarctica* Lipase B (CALB-T2-150) was obtained from ChiralVision. Most of the solvent used was purchased from Merck.

Formulation of nanoemulsion system: Vegetable oils i.e. sunflower, olive, palm, and coconut oil were used as the carrier oil. They are commercial cooking oils obtained from a retail outlet. Surfactants i.e. Tween-80 (Tw-80), Span-80 (Sp-80) and Chremophor EL (CrEL) were purchased from Sigma-Aldrich. The HLB value for Tween-80, Span-80 and Chremophor EL are 15, 4.3 and 14; respectively. Ultrapure water was used as the aqueous phase.

3.2 Synthesis and recovery of glucose monooleate (GluO)

The reaction was done according to Ariffin et al., (2014) with slight modification. The synthesis of the ester was performed in ethyl methyl ketone as the reaction solvent. The substrate which consists of alkyl donor (oleic acid) and alkyl acceptor (D-glucose) was calculated at a mol ratio of 3:1 and the immobilized enzyme of *Candida antarctica* Lipase B used was 1 g per alkyl acceptor. Esterification was carried out at 35^0 C, 200 rpm agitation speed for 48 hours.

After the end of the reaction, the mixture was filtered (using Whatman filter paper) into a separatory funnel to remove the immobilized enzyme lipase and non-dissolved D-glucose. Ultrapure water was added to the mixture and vigorously mixed to solubilize unreacted D-glucose residue. The mixture was allowed to stand until two separate liquid layers formed and the lower layer that consisted of water and residual D-glucose was removed. The procedure was repeated more than 5 times. The upper layer which consisted of the sugar-fatty acid ester (glucose monooleate – GluO) and unreacted oleic acid was then subjected to evaporation at 80^0 C overnight to remove the ethyl methyl ketone.

After the evaporation process, the mixture was allowed to cool down at room temperature until the GluO formed an amorphous glassy state within the oleic acid. The mixture was then subjected to centrifugation at 10, 000 x g for 30 minutes until two separate layers had formed. The upper layer that consisted of free oleic acid was removed.

3.3   Authentication of glucose monooleate (GluO)

The recovered GluO (technical grade) with a physical characteristic of an amorphous glassy state and yellowish appearance was sampled out and analyzed using Fourier-transform infrared (FTIR) along with proton nuclear magnetic resonance (^{1}H-NMR) to verify the final product formation. Prior to that, the product was extensively dried in a vacuum oven over diphosphorus pentoxide overnight.

The FTIR spectrophotometer (Spectrum 400, Perkin-Elmer, USA) in the wavenumber range of $500 - 4000$ cm^{-1} was used to analyze the functional group. The machine is equipped with PIKE GladiATR hovering monolithic diamond ATR accessory (Pike Technologies Inc., USA). While for ^{1}H-NMR, the product was dissolved in methanol-d$_4$ with a final concentration of 5mg/ml following previous study (Ishak et. al., 2019). The NMR spectroscopy machine is JEOL JNM-GSX 270 FT-NMR spectrometer (JOEL, Tokyo, Japan) operated at 400 MHz.

3.4 Preparation of O/W nanoemulsion through PIC method

Oil-in-water (O/W) nanoemulsion was prepared using the phase inversion composition (PIC) method. The organic phase which consists of surfactants (S) and vegetable oil (O) were mixed at room temperature (25 ± 1 °C) in a microcentrifuge tube. Ultrapure water (W) was added dropwise into the organic mixture (surfactants, S and oil, O) with constant stirring until the system is hydrated with excess water i.e. 90 % w/w of total emulsion solution. Different ratios of surfactant-to-oil (S:O) and will be tested to study their efficiency in nanoemulsion formation against different types of vegetable oils which will act as the carrier oil. Each formulation was prepared in duplicate to ensure consistency and store at room temperature.

Different vegetable oil was screened using a single surfactant which is Tw-80, Sp-80 and synthesized GluO to compare their ability in the emulsification (Table 3.1).

Table 3.1: Screening of single surfactants in a different composition of S:O ratio.

Surfactants	Vegetable oil	S:O Ratio
Tw-80	Sunflower, Olive, Coconut and Palm oil	100:0, 90:10, 80:20 and 70:30
Sp-80	Sunflower, Olive, Coconut and Palm oil	100:0, 90:10, 80:20 and 70:30
GluO	Sunflower, Olive, Coconut and Palm oil	100:0, 90:10, 80:20 and 70:30

In addition, the influence of CrEL as co-surfactant to Tw-80, Sp-80 and GluO in the formation of O/W nanoemulsion was studied. Surfactant (S) fraction of CrEL and Tw-80, Sp-80 or GluO was fixed at 63:37 based on previous literature (Ishak & Annuar, 2017). The surfactant mixtures were tested on sunflower oil at different S:O ratio as described in Table 3.2.

Table 3.2: Surfactant mixture in different S:O ratios.

CrEL: Surfactant (63:37)	Vegetable oil	S:O Ratio
CrEL: Tw-80	Sunflower oil	100:0, 90:10, 80:20, 70:30, 60:40, 50:50 and 40:60
CrEL: Sp-80	Sunflower oil	100:0, 90:10, 80:20, 70:30, 60:40, 50:50 and 40:60
CrEL: GluO	Sunflower oil	100:0, 90:10, 80:20, 70:30, 60:40, 50:50 and 40:60

3.5   Characterization of particle size and distribution

The size and size distribution of droplets was measured by a dynamic light scattering (DLS) technique using a Zetasizer-nanoseries (ZEN3600, Malvern Instruments Ltd, UK) by diluting 100µl of the sample with 900µl of ultrapure water to avoid multiple scattering effects.

3.6   Visual observation of emulsion

The appearance of the resulted emulsion was recorded based on the following visual observation (Table.3.3).

Table 3.3: Categories of visual observation.

Category	Description
Coarse emulsion	Milky and cloudy mixture
Nanoemulsion	Clear and transparent / translucent mixture

3.7   Emulsion morphology study

The morphology of nanoemulsion samples was observed using OPM (BX51, Olympus, Japan) to detect the presence of birefringence, which indicates the existence of a well-ordered molecular structure. All samples were placed on a glass slide and covered with glass slip. Then, a small amount of ultrapure water was dropped at the edge of coverslip to allow water penetration through capillary action. After 20-30 minutes, all samples were observed under polarized light and images were captured using a digital camera (DP26, Olympus, Japan) and analyzed using cellSens-standard software. The image was captured using under the magnification factor of 10, 20 or 50.

The SAX scattering was conducted to investigate the presence of ordered structure in the emulsion sample using an X-ray instrument (SaxSpace, Anton Paar, Austria). All measurements were performed using line collimation with an exposure time of 15 minutes. Samples were fully loaded into a paste cell holder for measurement. X-ray patterns were recorded using 1-D diode detector under vacuum at 25 ^{0}C. The obtained data was analyzed using SAXSquant and SGI software package.

The FTIR analysis was conducted to investigate the intermolecular interaction of the emulsion system at different water contents. Measurement was done using FTIR spectrophotometer (Spectrum 400, Perkin-Elmer, USA) at the range of 500 - 4000 cm^{-1} wavelength.

CHAPTER 4: RESULTS AND DISCUSSION

4.1   Authentication of Glucose monooleate (GluO) formation

The reaction of D- glucose with oleic acid was done through enzymatic esterification reaction as depicted in Figure 4.1. The final product was then authenticated by using Fourier-transform infrared (FTIR) analysis and proton nuclear magnetic resonance (^{1}H-NMR) to confirm the formation of the sugar fatty ester.
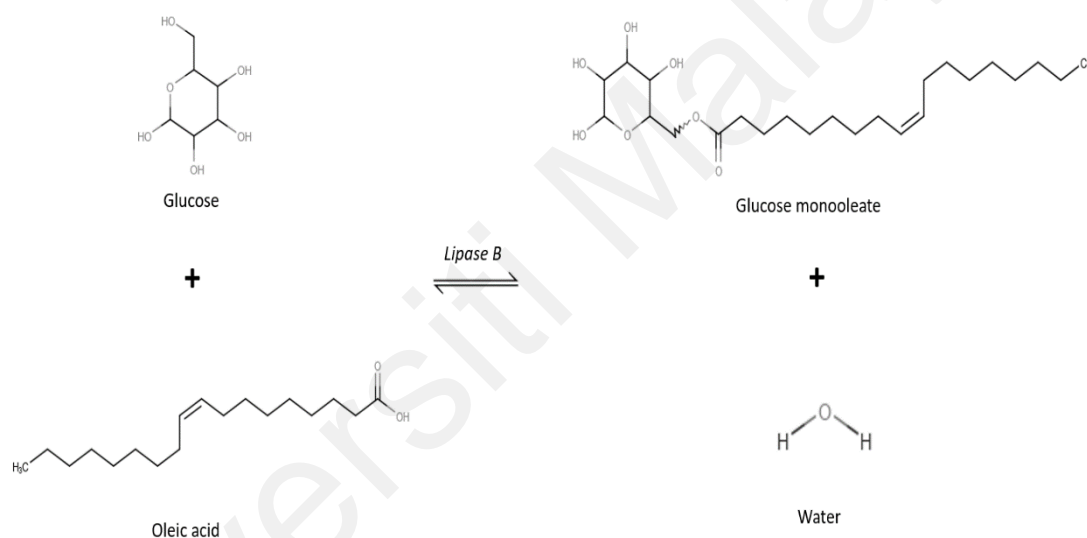
Figure 4.1: Lipase-catalyzed esterification of D-glucose with oleic acid.

The FTIR spectrum of individual starting materials utilized for the formation of GluO was obtained as in Figure 4.2. The spectra of D-glucose monohydrate used in this study shows the absorption band at 3300 cm^{-1}, and 1050 cm^{-1} correspond to -OH and C-O-C bond that is normally presented in glucose structure (Figure 4.2a). The FTIR spectra of oleic acid show absorption band at 2900 cm^{-1}, 2850 cm^{-1}, 1700 cm^{-1} and 1650 cm^{-1} correspond to CH$_2$, CH$_3$, C=O and C=C bond that is normally presented in oleic acid

structure (Figure 4.2b). The FTIR spectra of the product confirm the formation of GluO based on the vibration absorbance of -OH (3300 cm^{-1}) and C-O-C (1050 cm^{-1}) along with CH$_2$ (2900 cm^{-1}), CH$_3$ (2850 cm^{-1}), C=O (1700 cm^{-1}) C=C (1650 cm^{-1}) that intersect with spectra of D-glucose monohydrate and oleic acid while the absorption band at 1100 cm^{-1} indicates ester bond O=C-O-CH$_2$ that is not present in spectra of both glucose and oleic acid (Figure 4.2c).
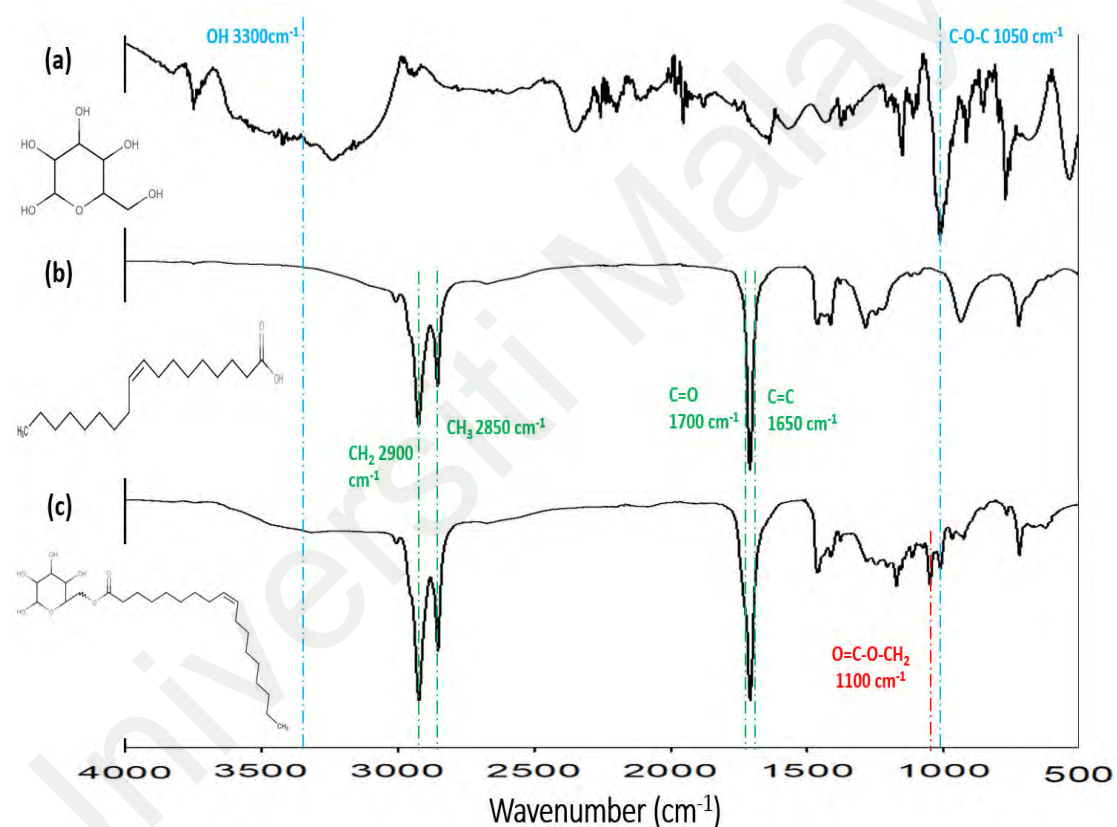
Figure 4.2: FTIR spectra of (a) D-glucose, (b) oleic acid and (c) GluO.

Figure 4.3 displays the ^{1}H-NMR spectra for the product (GluO). The spectrum shows the characteristics of oleic acid esterified with a glucose molecule. The peak of protons at ≈ 0.9 ppm represents the CH$_3$ oleic acid terminal end. The repeating units of CH$_2$

oleic acid carbon atom is represented by the proton peak at ≈ 1.35 ppm while proton peak at ≈ 1.63 ppm represents the C_3 of oleic acid. The proton shifts of CH_2 oleic acid functional end from 2.31 to 2.35 (from e to e*) indicates chemical shift due to the esterification of oleic acid with glucose (Ren & Lamsal, 2017). The peaks of proton double bond, which indicates the unsaturated carbon chain of oleic acid was detected at ≈ 5.35 ppm. The presence of a double bond affects the chemical shift of first CH_2 neighbours of the protons which represented by the peak at ≈ 2.05 ppm. These proton peaks are comparable with existing literature of NMR characterization of sugar fatty acid esters (Ren & Lamsal, 2017).
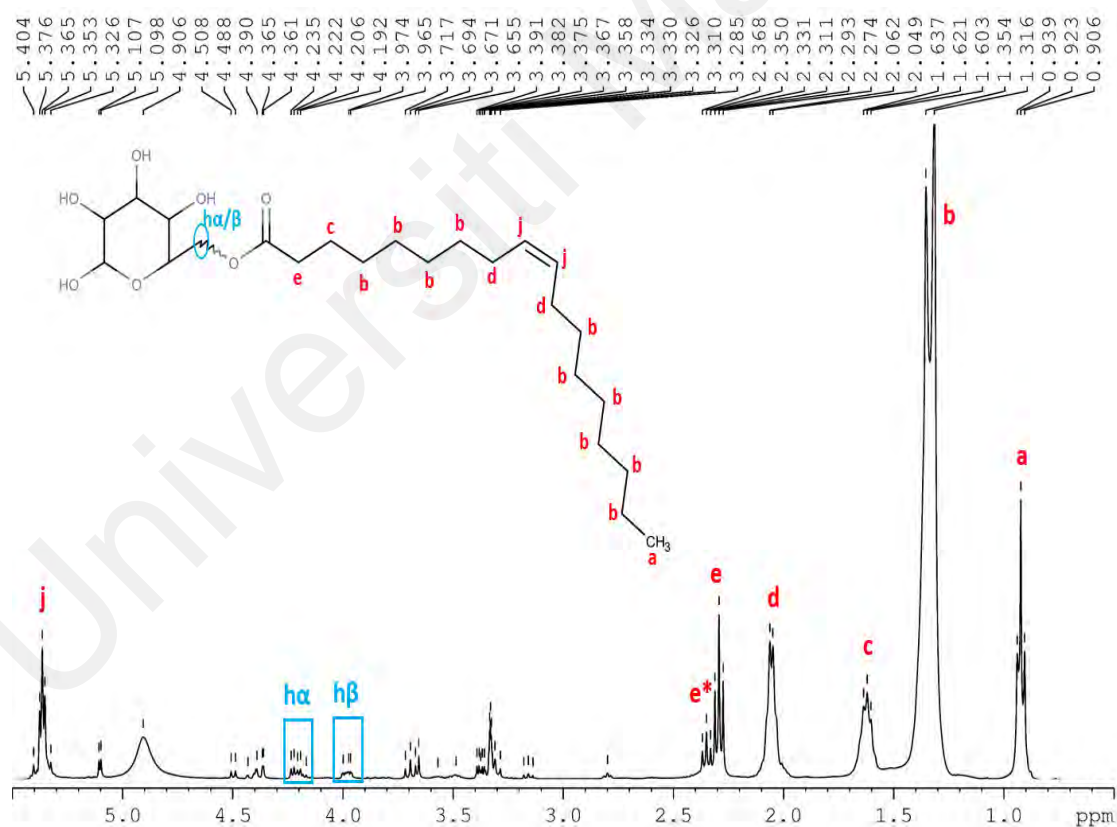
Figure 4.3: Proton H NMR of Glucose monooleate (GluO).

The proton NMR spectrum for D-glucose was observed at different peaks. The proton peaks at $\approx$ 3.39 to 5.1 ppm are in accordance with NMR characterization of D-glucose (Ren & Lamsal, 2017). Two chemical shifts detected at $\approx$ 4.23 and $\approx$ 3.95 ppm indicating the alpha (α) and beta (β) conformation of the glucose-fatty acid ester bond. The α- and β-anomeric forms of sugar head was detected at $\approx$ 5.1 and $\approx$ 4.5 respectively.

4.2 Preparation of O/W nanoemulsion through PIC method

4.2.1 Single surfactant system

The selection of surfactants is a critical consideration in the construction of the emulsification system. Each surfactant has a specific HLB value that determines the final solubilization and stability of the emulsification system (Ishak & Annuar, 2017; Mahdi et al., 2011). Tw-80 and Sp-80 are used as a comparison to the synthesized product i.e. GluO, in their ability to form nanoemulsion in different types of vegetable oils. These surfactants are categorized as non-ionic surfactants and shared the same hydrophobic part that consists of long oleoyl (C18:1) hydrocarbon chain. The similar structure of the hydrophobic region of Tw-80 and Sp-80 make them suitable comparative candidates to further understand the nature of GluO in the formation of nanoemulsion.

Tween-80 (Tw-80) is a hydrophilic surfactant with an HLB value of 15 that consists of bulky polyoxyethylene group as hydrophilic head and oleic acid chain as the hydrophobic tail. The FTIR spectra shows the vibration absorbance of -OH (3300 cm^{-1}), CH$_2$ (2800-2900 cm^{-1}), C=O (1700 cm^{-1}) C=C (1650 cm^{-1}) and C-O-C (1100 cm^{-1}) as

shown in Figure 4.4a. Meanwhile, Sp-80 is a hydrophobic surfactant with an HLB value around 4.3 that consists of a sorbitan ring as hydrophilic head and oleic acid chain as the hydrophobic tail. The FTIR spectra shows the vibration absorbance of -OH (3300 cm^{-1}), CH_2 (2800-2900 cm^{-1}), C=O (1700 cm^{-1}) C=C (1650 cm^{-1}), C-O-H (1200 cm^{-1}) and C-O-C (1100 cm^{-1}) as in Figure 4.4b. While for GluO, the FTIR spectra shows the vibration absorbance of -OH (3300 cm^{-1}), CH_2 (2800-2900 cm^{-1}), C=O (1700 cm^{-1}) C=C (1650 cm^{-1}), C-O-H (1200 cm^{-1}) and C-O-C (1100 cm^{-1}) as in Figure 4.4c.
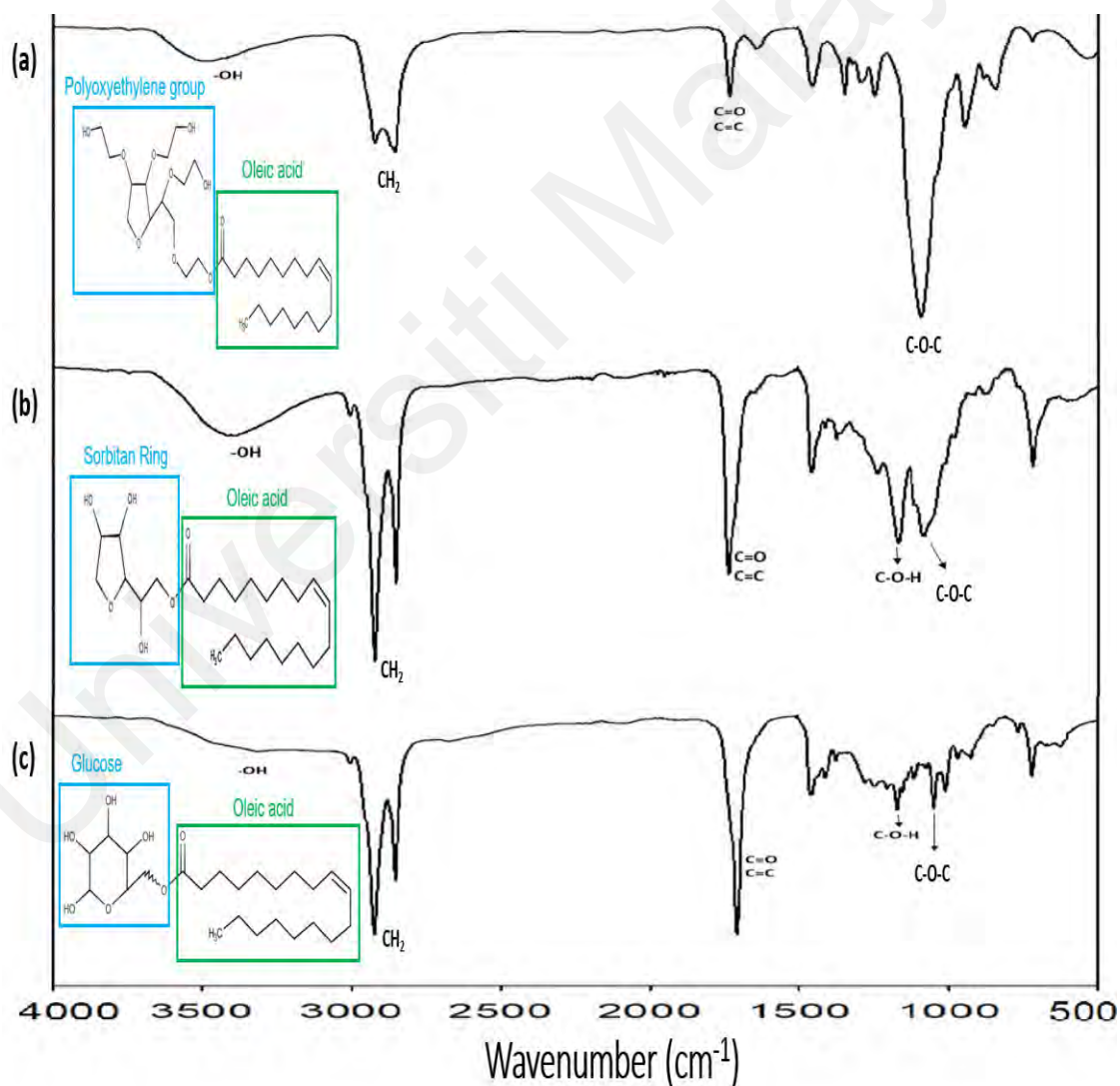
Figure 4.4: FTIR spectra of (a) Tween-80, (b) Span-80 and (c) Glucose monooleate.

Figure 4.5 shows the screening result of the surfactant of Tw-80, Sp-80 and GluO in the absence of carrier (vegetable) oil at 90 % water content. Tween-80 (Tw-80) gave the smallest droplet with an average size of 10.3 ± 0.43 nm. Visual observation showed the solution was transparent and flowable. Meanwhile, Sp-80 and GluO showed poor solubilization capacity in the absence of carrier oil and both surfactants tend to aggregate in the presence of water. Visual observation showed the solutions were cloudy and milky indicating the presence of large particle aggregates. The average particle size was determined at more than 1 µm for both Sp-80 and GluO.
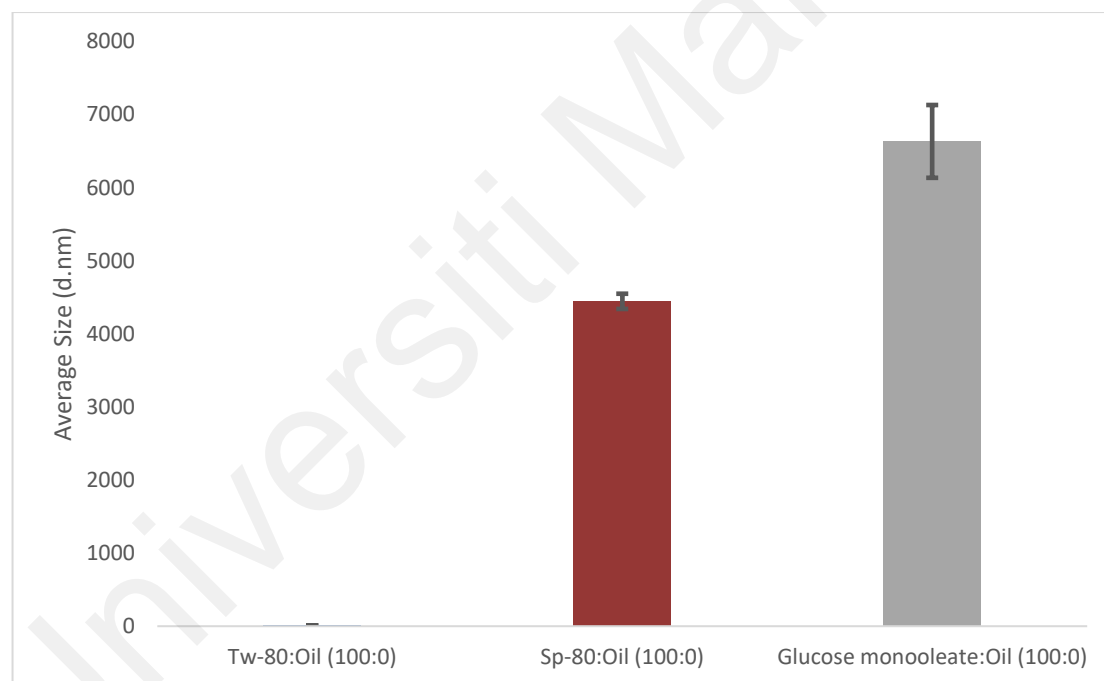
Figure 4.5: Average size of surfactants particle (without carrier oil i.e. S:O = 100:0) at 90 % water content.

Figure 4.6 shows the screening result of Tw-80, Sp-80 and GluO at different S:O ratio starting from 90:10, 80:20 and 70:30 in different vegetable oils (sunflower, olive, palm and coconut oil) with 90 % of water content. From the graph, Tw-80 shows high

solubilization capacity in different ratios of S:O in all types of vegetable oils compared to Sp-80 and GluO. At surfactant-to-oil ratio (S:O) of 90:10, Tw-80 could form nanoemulsion in all types of oils with an average droplet size ranging from 12.6 nm to 17.1 nm. Visual observation also indicated that the solution was transparent and flowable at 90 % water content. Meanwhile, Sp-80 and GluO showed weak solubilization capacity at the same S:O ratio (90:10) in all types of vegetable oils (Figure 4.6a). However, the size of particle aggregation was significantly reduced in the presence of carrier oils as compared to without oil incorporation (Figure 4.5). Visual observation showed that all mixture was cloudy and milky indicating the formation of a coarse emulsion. As the oil content gradually increased to 20 and 30 % w/w of the organic mixture, the average droplet size of Tw-80 increased exponentially with the maximum average size was observed at 586.9 ± 74.8 nm (Figure 4.6b and c). At this point, the mixture tends to show cloudy and milky behaviour. In contrast, Sp-80 and GluO showed a significant decrease in the droplet size with increasing oil content at 20 and 30 % in all types of vegetable oils (Figure 4.6b and c). However, the emulsion formed by these two surfactants is still categorized as a coarse emulsion with an average size of more than 1 μm. All the mixture exhibited cloudy and milky characteristics.

The Tw-80 showed the highest solubilization capacity compared to other Tween series such as Tw-20, Tw-60 and Tw-85 (Mahdi et al., 2011). It is suggested that the hydrophobic part, which consists of unsaturated long-chain carbon tail (C18:1) of oleic acid, provides strong interaction between different types of vegetable oils that maintain the nano-sized oil-swollen micelle in the presence of water.
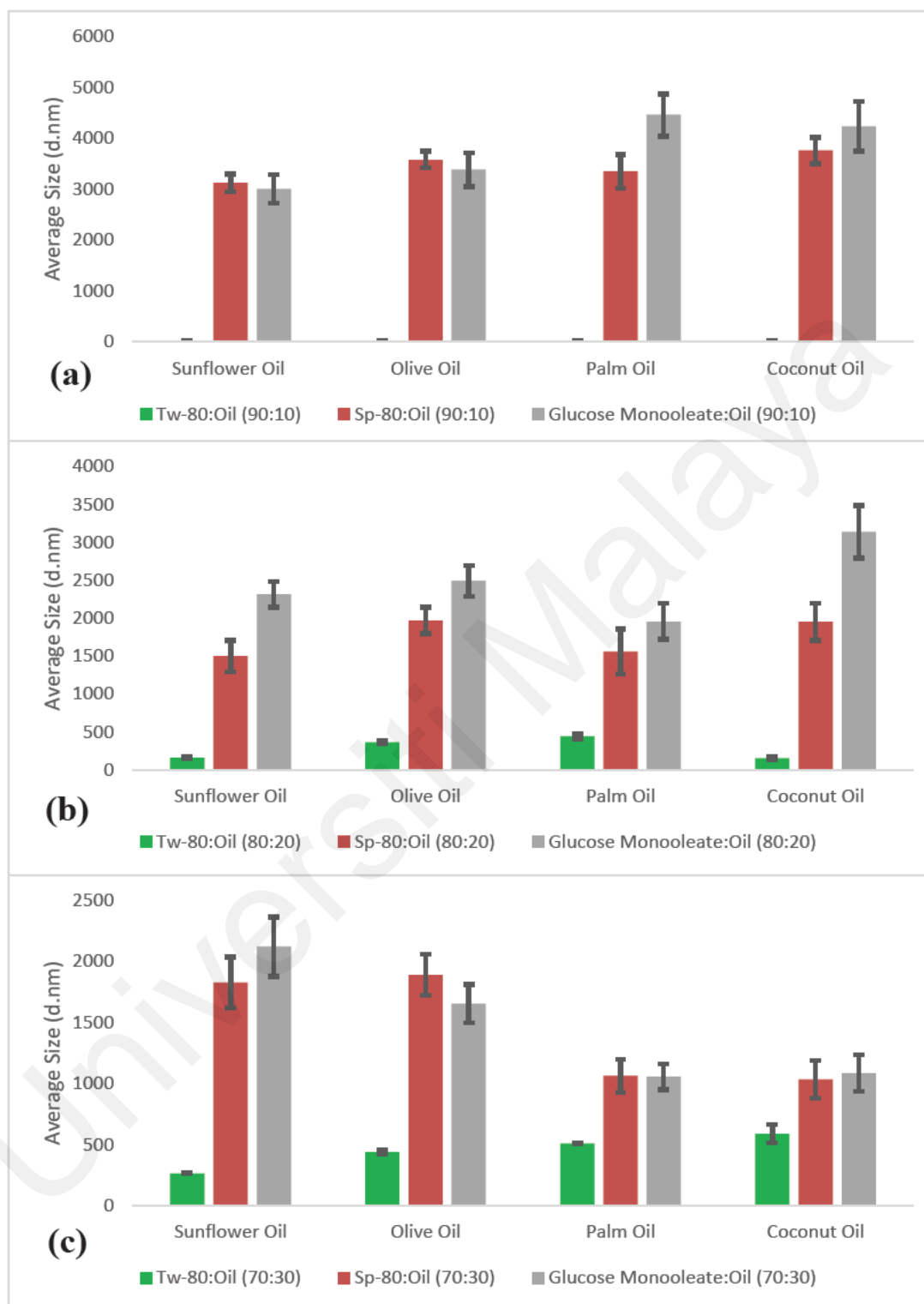
Figure 4.6: Average size of formed oil droplets at different S:O and vegetable oils. Water content is at 90 % w/w.

The result of Sp-80 screening was as expected as it is a lipophilic surfactant. In the presence of water, Sp-80 showed poor solubility and tend to aggregate, which will result in a coarse emulsion. The sorbitan ring is less soluble in water due to less hydroxyl group as compared to Tween series with large polyoxyethylene head group. These explain the reason why Sp-80 showed poor solubility in the presence of water. It is expected that the glucose head of GluO that replaces the sorbitan ring would have higher hydrophilicity than Sp-80, thus may perform better solubilization of oil in the presence of water. This expectation is based on the fact that glucose has more hydroxyl groups than sorbitan ring. However, the use of GluO as a single surfactant to form nanoemulsion through phase inversion composition technique cannot be achieved. This indicates that GluO has almost similar lipophilicity property as Sp-80.

From the preliminary screening of single surfactant system, it can be concluded that Tw-80 was able to form oil droplets with a size of less than 100 nm at 90:10 of surfactant-to-oil ratio for all types of vegetable oils through phase inversion composition (PIC) technique. However, a single surfactant system of Sp-80 and GluO were not able to produce nanoemulsion through the same PIC technique. Proper selection of carrier oils, surfactants and cosurfactants along with their optimum concentration is crucial to obtain a stable nanoemulsion (Ishak & Annuar, 2017; Mahdi et al., 2011; Zeng et al., 2017).

4.2.2 Surfactant mixture system

Incorporation of co-surfactants can alter the emulsification efficiency of a particular surfactant and could synergistically enhance the dispersion and solubilization of the oil phase into smaller droplet sizes (Ishak et al., 2017; Zeng et al., 2017). Cremophor EL (CrEL) is another type of non-ionic surfactant with an HLB value between 12 to 14 that exists in a yellow liquid form at room (Figure 4.7) (Zeng et al., 2017). It has a good emulsifying capacity and thus widely used in pharmaceutical industries to encapsulate lipophilic drugs (Ishak et al., 2017; Ishak et al., 2019; Zeng et al., 2017). From a previous study, an optimized ratio of CrEL and Sp-80 (CrEL: Sp-80) for the formation of nanoemulsion through low energy method was 63:37 (Ishak & Annuar, 2017). Thus, the CrEL: Tw-80 / Sp-80 / GluO ratio of 63:37 was used in this study.
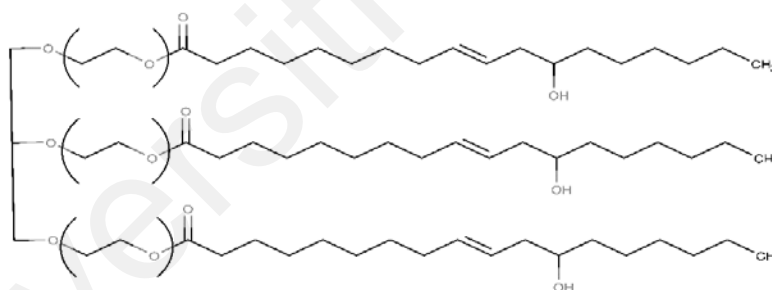
Figure 4.7: Structure of Cremophor EL (where x + y + z = 35).

Figure 4.8 shows the average droplet size for formulation contained fix 63:37 ratio of Cremophor EL (CrEL) and Tween 80 (Tw-80) but in different amount of sunflower oil i.e. 100:0, 90:10, 80:20, 70:30, 60:40, 50:50 and 40:60 of organic mixture ratio (surfactant-to-oil - S:O). The average size of droplet size tends to increase at increasing oil content. In the absence of oil, CrEL: Tw-80 (63:37) showed the smallest droplet size

$(12.6 \pm 0.9$ nm) with visual observation noted the mixture was transparent and flowable. As oil content is increased by 10 % w/w of the organic mixture, the average droplet size tends to grow larger at 52.7 ± 9.3 nm. At 20 % oil content and above, the average size was over 200 nm and the mixture start to show milky characteristics. At a higher S:O ratio, the surfactant mixture was not able to emulsify the oil efficiently to form nanoemulsion. This shows that the cut off oil content for CrEL: Tw-80 (63:37) was at 10 %.

Figure 4.8: Emulsions of sunflower oil at different S:O using surfactant mixture of CrEL and Tw-80 at ratio of 63:37.

Figure 4.9 shows the average droplet size for a formulation containing a mixture of CrEL and Span 80 (Sp80). The ratios of surfactant mixture and S:O are the same as

previous formulation. In the absence of oil, the average size droplets were 187.6 ±11.5 nm and in the presence of 10 % sunflower oil (w/w of organic mixture), the droplet size significantly decreases to 83.8 ± 5.9 nm and the mixture was slightly transparent by observation. As the oil content increased at 20 and 30 %, the average droplet size tends to further decrease in size at 26.9 ± 2.9 and 32.2 ±1.5 nm respectively. The mixtures were clear and transparent. However, starting at 40% oil content, the average droplet size started to increase gradually with increasing oil content. The highest average size observed was 159 ±20.4 nm at S:O ratio of 40:60.
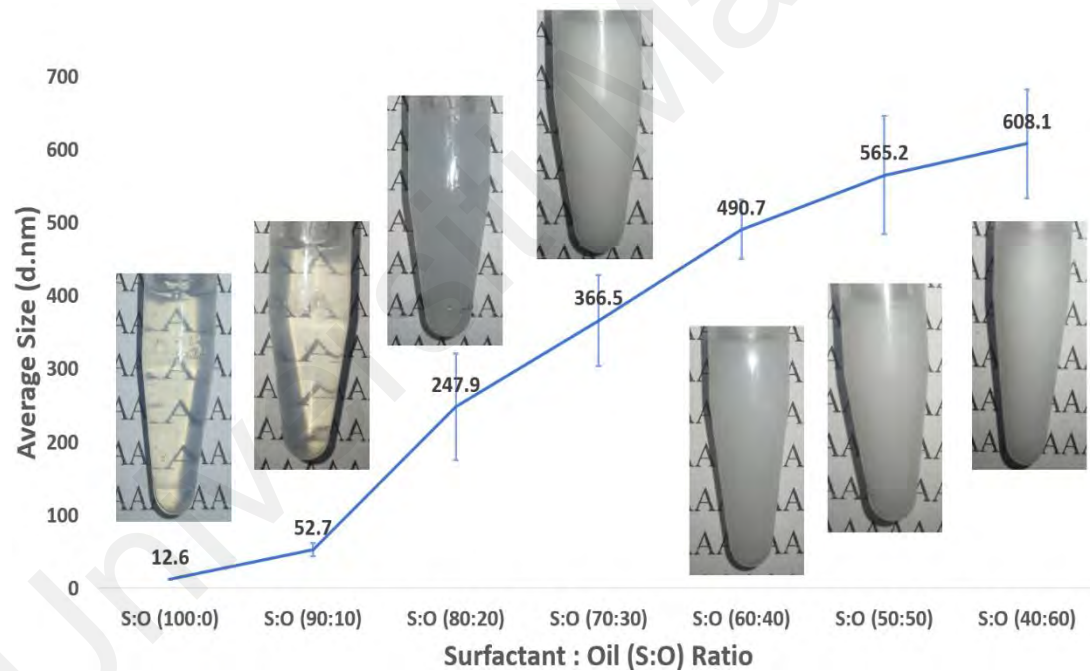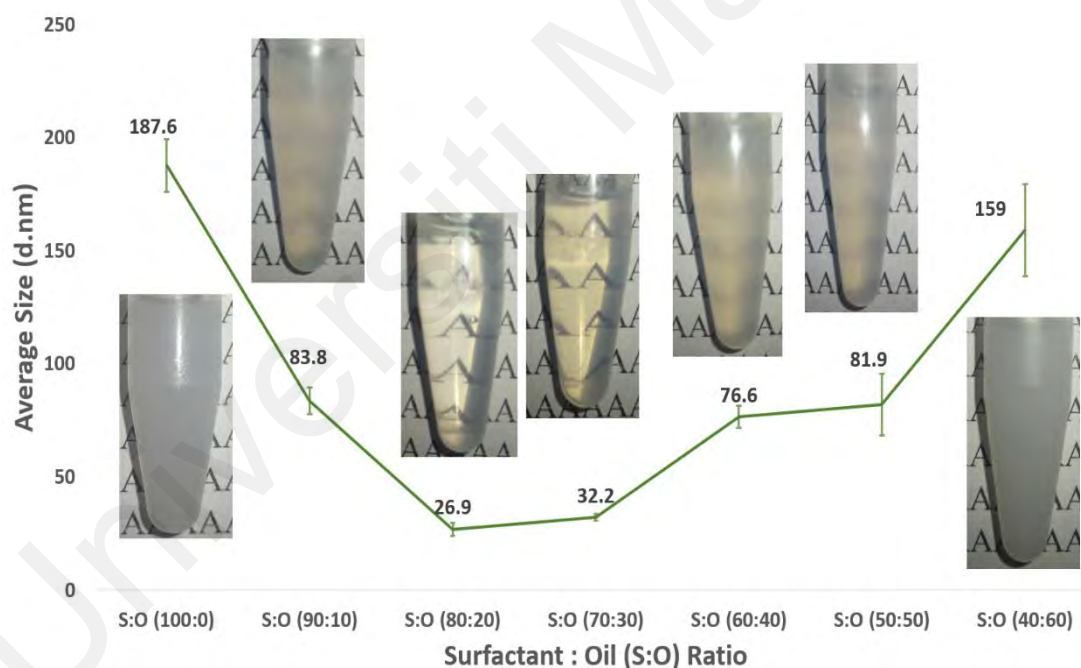

Figure 4.9: Emulsions of sunflower oil at different S:O using surfactant mixture of CrEL and Sp-80 at ratio of 63:37.

Figure 4.10 shows the average droplet size of emulsions formed by surfactant mixture of CrEL and glucose monooleate (GluO) at a ratio of 63:37 and different S:O starting

from 100:0, 90:10, 80:20, 70:30, 60:40, 50:50 and 40:60. Interestingly, the average size droplet decreased proportionally in size with increasing oil content. Initially, in the absence of oil, the surfactant mixture exhibited poor solubility in which the average droplet size was 316.5 ± 25.6 nm and the mixture was observed to be cloudy and milky characteristics. At 10 and 20 % oil content (w/w of organic mixture), the average droplet size became smaller at 206.2 ± 11.2 and 158.6 ± 23.2 nm respectively. As the oil content increased at 30 and 40 %, the average size droplet reduced drastically to 47.6 ± 4.5 and 40.3 ± 6.3 nm. At this point, the mixture showed transparent characteristics indicating the formation of nanoemulsion. However, at 50 % oil content, the average droplet size increased to 116.6 ± 15.5 nm and further increased to 197.6 ± 25.6 nm at 60 % oil content.

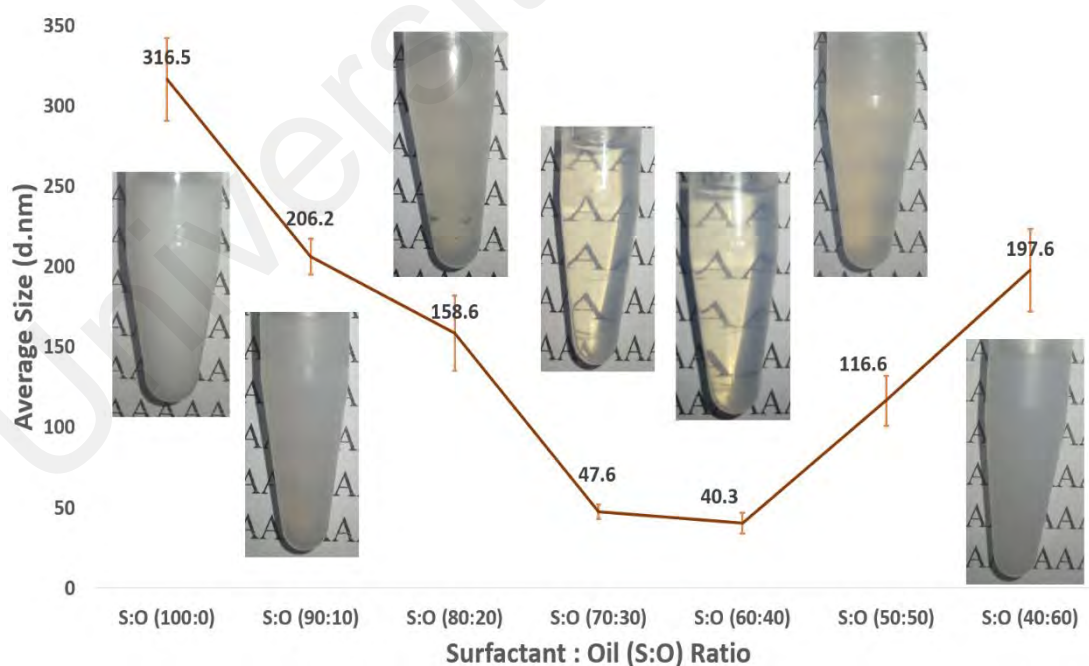**Figure 4.10: Emulsions of sunflower oil at different S:O using surfactant mixture of CrEL and GluO at ratio of 63:37.**

The incorporation of CrEL, along with GluO, proved that the mixture was able to form nanoemulsion at S:O ratio at 70:30 and 60:40 (Figure 4.10). HLB value of surfactants plays a vital role that influences the stability of the oil-water emulsion system (Perazzo et al., 2015). The incorporation of CrEL with Tw-80 was not able to stabilize the emulsion system at high oil content in which it produces coarse emulsion (Figure 4.8). Both CrEL and Tw-80 have a high HLB value of 12-14 and 15 respectively. In contrast to that, Sp-80 have a lower HLB value of 4.3. When it is incorporated with CrEL, the surfactant mixture was able to solubilize and stabilize the emulsion system at higher oil content and the same applies to GluO-incorporated CrEL mixture (Figure 4.9 and 4.10). Thus, the high differences of HLB values between two surfactants result in better solubilization efficiency that will result in the formation of nanoemulsion (Mahdi et al., 2011).

4.2.3   Effects of different types of vegetables oil

Based on the previous result, S:O ratio was fixed at 60:40 to determine the efficiency of surfactant mixture i.e. CrEL and Tw-80 / Sp-80 / GluO, in the formation of O/W nanoemulsion using different types of vegetable oils that are sunflower, olive, palm, and coconut oil. Table 4.1 summarize the resulted oil droplet size of the different formulations.

For CrEL/Tw-80 mixture, nanoemulsion was not formed in all types of vegetable oils. All mixtures exhibited cloudy and milky characteristics. The lowest oil droplet size obtained with sunflower oil (490.7 ± 40.2 nm), followed by coconut oil (671.2 ± 39.2 nm) while for olive oil and palm oil the average droplet size was more than 1.0 μm.

54

As for CrEL/Sp-80 mixture with the same S:O ratio as above, all mixture exhibited better solubilization of oil compares to previous surfactant mixture. The lowest oil droplet size obtained with sunflower oil (76.7 ± 4.8 nm) and coconut oil (94.8 ± 1.7 nm) followed by olive oil (195.8 ± 75.0 nm). The largest oil droplet size was obtained with palm oil in which the size is 216.6 ± 39.7 nm.

Meanwhile, CrEL/GluO mixture has the ability to form nanoemulsions in both sunflower oil and coconut oil with the average droplet size of 40.3 ± 6.3 and 31.9 ± 0.7 nm respectively. The appearances of the emulsion systems are clear and transparent as depicted in Table 4.1. For olive and palm oil, the average oil droplet size was 204.3 ± 56.7 and 221.8 ± 45.4 nm, respectively and the emulsions exhibiting cloudy characteristics i.e. coarse emulsion.

Table 4.1: Effects of vegetables oil[a] and surfactants mixture[b] on the size of oil droplet. The ratio of surfactant mixture and S:O are 63:37 and 60:40, respectively.

a / b	Sunflower Oil	Olive Oil	Palm Oil	Coconut Oil
CrEL:Tw-80	490.7 ± 40.2 nm	1726.5 ± 122.6 nm	1229.6 ± 161.6 nm	671.2 ± 39.2 nm
CrEL:Sp-80	76.7 ± 4.8 nm	195.8 ± 75.0 nm	216.6 ± 39.7 nm	94.8 ± 1.7 nm
CrEL:GluO	40.3 ± 6.3 nm	204.3 ± 56.7 nm	221.8 ± 45.4 nm	31.9 ± 0.7 nm

This result shows that the types of carrier oil used are also important parameters to be considered to produce nanoemulsion through phase inversion composition (PIC) technique (Perazzo et al., 2015). The surfactant-to-oil (S:O) ratio is not the only factor that will determine the fate of the droplet size and the stability of the oil-water emulsion, but rather, the degree of similarity between fatty chains of carrier oil and hydrophobic tail of surfactants may also influence the stability of the emulsion system (Mahdi et al., 2011).

From Table 4.1, it can be seen that the surfactant mixture of CrEL with Tw-80, Sp-80 and GluO has better solubilization of sunflower and coconut oil as compared to olive and palm oil. The composition and characteristics of each oil may influence the formation of droplet size in the surfactant mixture. However, a study presumed that there is no strong correlation between the size of droplets formed and the physicochemical characteristics of oil used in the emulsification system (Komaiko & Mcclements, 2016). Further study should be conducted to further understand the mechanism of emulsification in various types of carrier oils.

4.3   Emulsion Morphology Study

4.3.1   Optical polarized microscopy (OPM)

Microscopy images of phase inversion emulsification of different vegetable oils using different surfactant mixtures i.e. CrEL with Tw-80 or Sp-80 or GluO are shown in Figure 4.11 – 4.13. The ratio of surfactant mixture and S:O are 63:37 and 60:40, respectively. By using the surfactant mixture of CrEL/Tw-80, there was no birefringence region detected in all samples containing different vegetable oils. This indicates no formation of a well-ordered structure within the samples upon water penetration.

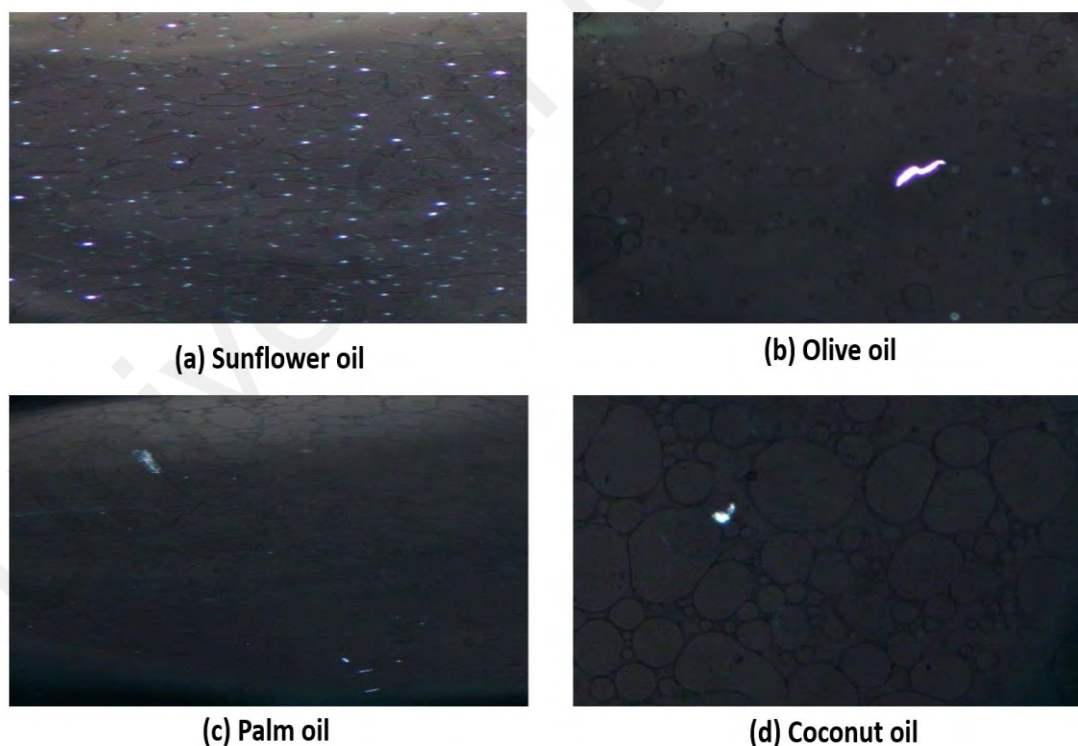(a) Sunflower oil   (b) Olive oil

(c) Palm oil   (d) Coconut oil

Figure 4.11: Optical polarized microscopy (OPM) images of a hydrated ternary-phase system consisting of CrEL/Tw-80 with different vegetable oils. The ratio of surfactant mixture and S:O are 63:37 and 60:40, respectively.

In contrast, the presence of birefringence region in samples containing sunflower (Figure 4.12a and 4.13a) and coconut oil (Figure 4.12d and 4.13d) was detected when surfactant mixture of CrEL/Sp-80 and CrEL/GluO were used. However, no birefringence was detected in samples containing olive (Figure 4.12b and 4.13b) and palm oil (Figure 4.12c and 4.13c). The presence of a birefringence region indicating the formation of a well-ordered structure in the samples upon water addition.

Birefringence is an optical property of a material having more than two refractive indices that depend on the propagation and polarization of light (Hindi, 2016). The image observed using an optical polarizing microscope (OPM) in a water penetration study can verify the formation of an anisotropic structure during the emulsification process. The anisotropic structures such as lamellar and hexagonal and can show birefringence features that may give rise to vibrant image and colour. Theoretically, the formation of nanoemulsion through PIC method requires the formation of a bi-continuous/lamellar structure at emulsion inversion point (EIP) before it is dispersed into fine oil droplets with further addition of water (Perazzo et al., 2015; Roger, 2016). This bi-continuous/lamellar structure formation indicates balanced intermolecular interaction among water, oil and surfactant and it is an anisotropic structure that shows birefringence characteristics when observed under cross-polarized light using OPM. Without the proper formation of a bi-continuous/lamellar structure at emulsion inversion emulsion point (EIP), the oil cannot be gradually dispersed into nano-sized droplets (Ishak & Annuar, 2016, 2017). Therefore, samples with surfactant mixtures of CrEL/Sp-80 and CrEL/GluO in sunflower and coconut oil were able to form bi-continous/lamellar structure during emulsification since they produced emulsion system

58

with the size of oil droplet less than 100 nm (Table 4.1). This is supported with the OPM

images that show the presence of birefringence region in those samples during water

penetration study (Figure 4.12a & d and Figure 4.13a & d).

(a) Sunflower oil

(b) Olive oil

(c) Palm oil

(d) Coconut oil
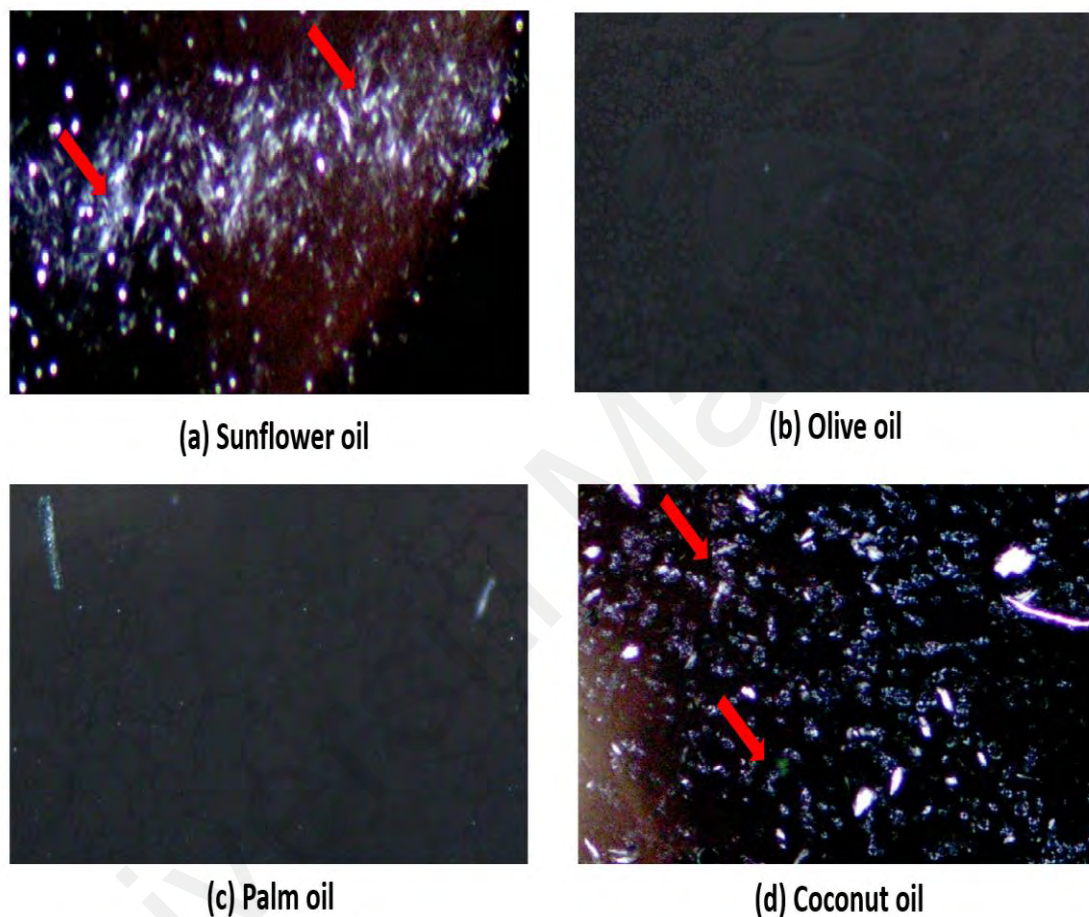
Figure 4.12: Optical polarized microscopy (OPM) images of a hydrated ternary-phase system consisting of CrEL/Sp-80 with different vegetable oils. The ratio of surfactant mixture and S:O are 63:37 and 60:40, respectively. Arrows show the presence of birefringence.
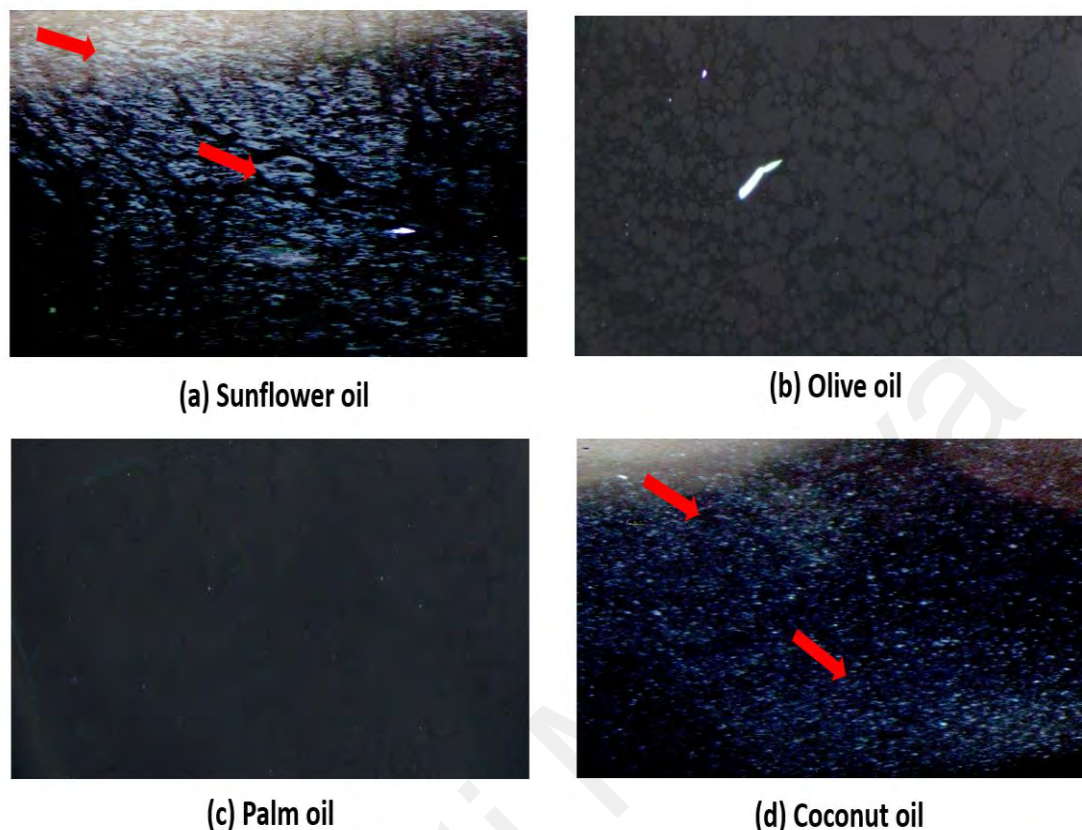
Figure 4.13: Optical polarized microscopy (OPM) images of a hydrated ternary-phase system consisting of CrEL/GluO with different vegetable oils. The ratio of surfactant mixture and S:O are 63:37 and 60:40, respectively. Arrows show the presence of birefringence.

4.3.2 Fourier-transform infrared (FTIR) analysis

The intermolecular interaction among components in the emulsion system based on the changes in functional group spectra at different water contents was studied using FTIR. The ratio of surfactant mixture (CrEL with Tw-80 / Sp-80 / GluO) and S:O were fixed at 63:37 and 60:40, respectively but the water content was varied from 20 – 50 % w/w. In general, all three components of mixed surfactant (CrEL with Tw-80 / Sp-80 / GluO) shared a similar peak of chemical bonds representing -OH (3300 cm^{-1}), CH$_2$ (2800-2900 cm^{-1}), C=O (1700 cm^{-1}), C=C (1650 cm^{-1}), C-O-C (1100 cm^{-1}), and a single

broad peak exist with the addition of water indicating C-H bend (700 cm^{-1}) as in Figure 4.14a, 4.15a and 4.16a.

Figure 4.14: The FTIR spectra of ternary-phase system consisting CrEL/Tw-80 (63:37) and sunflower oil at different water content of (a) 20, (b) 30, (c) 40 and (d) 50 % w/w.

Figure 4.14 shows spectral information of ternary-phase system containing mixed surfactants of CrEL/Tw-80 (63:37) at different water content starting from 20 to 50%. At 40% water content (Figure 4.14 c), the absorbance of CH$_2$ (2800-2900 cm^{-1}), C=O (1700 cm^{-1}) C=C (1650 cm^{-1}) C-O-C (1100 cm^{-1}) and C-H bend (700 cm^{-1}) were not aligned indicating no formation of bi-continuous microemulsion during the emulsification process. Furthermore, a sudden increase of -OH absorbance (3300 cm^{-1}) at 50 % water content was identified (Figure 4.14 d), which indicates that phase inversion from W/O to O/W emulsion has occurred around this region.

Figure 4.15: The FTIR spectra of ternary-phase system consisting CrEL/Sp-80 (63:37) and sunflower oil at different water content of (a) 20, (b) 30, (c) 40 and (d) 50 % w/w.

Figure 4.15 shows spectral information of ternary-phase system containing mixed surfactants of CrEL/Sp-80 (63:37) in sunflower oil (60:40 of surfactant-to-oil ratio) at different water content starting from 20 to 50 %. Unlike the previous system containing CrEL/Tw-80, the -OH absorbance (3300 cm^{-1}) of this system went through gradual increments with the increasing amount of water composition. Furthermore, the peaks representing CH$_2$ (2800 -2900 cm^{-1}), C=O (1700 cm^{-1}), C-O-C (1100 cm^{-1}) and C-H bend (700 cm^{-1}) showed almost similar value of transmittance at 40 % water content suggesting the formation of lamellar/bi-continuous microemulsion whereby surfactant molecules aligned themselves in between oil-water phase stream at minimum interfacial tension. This indicates that the phase inversion point for the formulated sample occurred at 40 % water content. Similar peak pattern changes were observed on the system

containing mixed surfactant of CrEL/GluO (Figure 4.16). Therefore, the formation of lamellar/bi-continuous microemulsion at inversion point was also suggested to occur in the system as well.
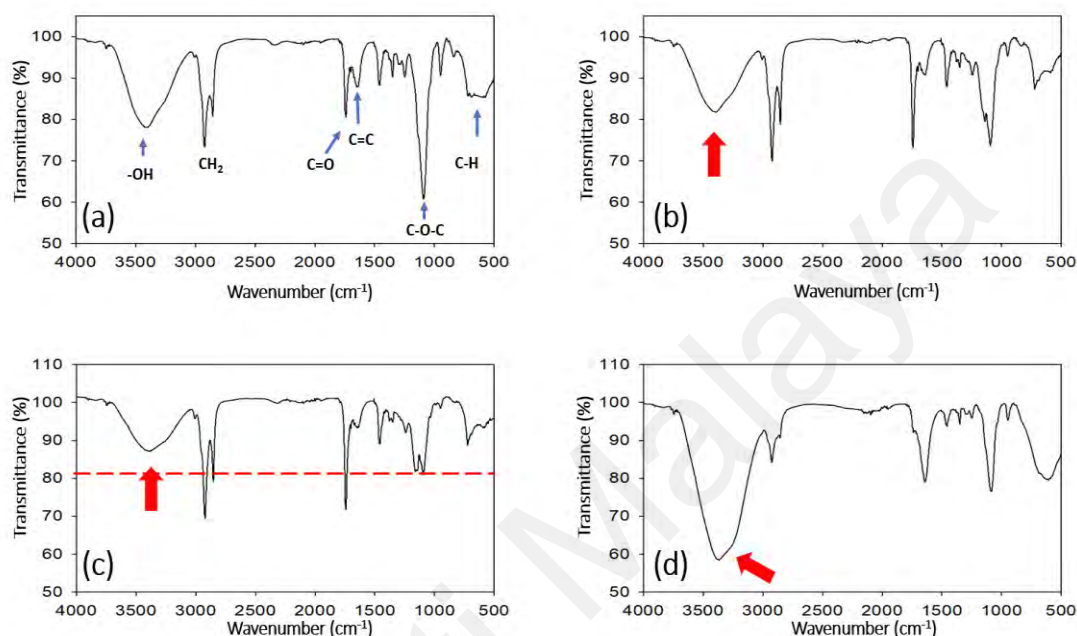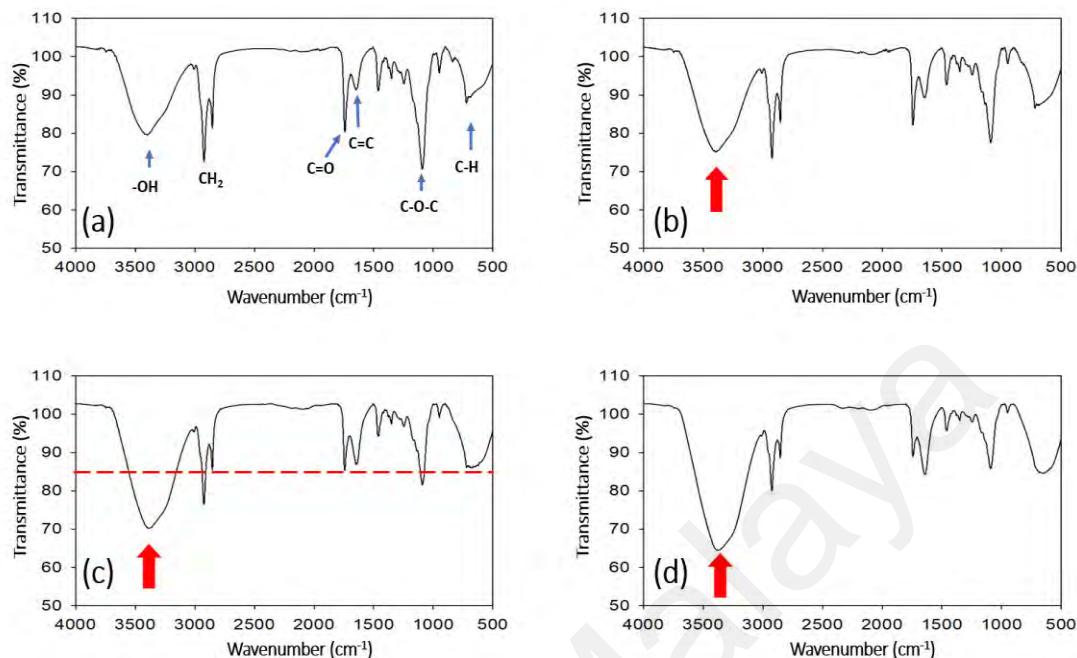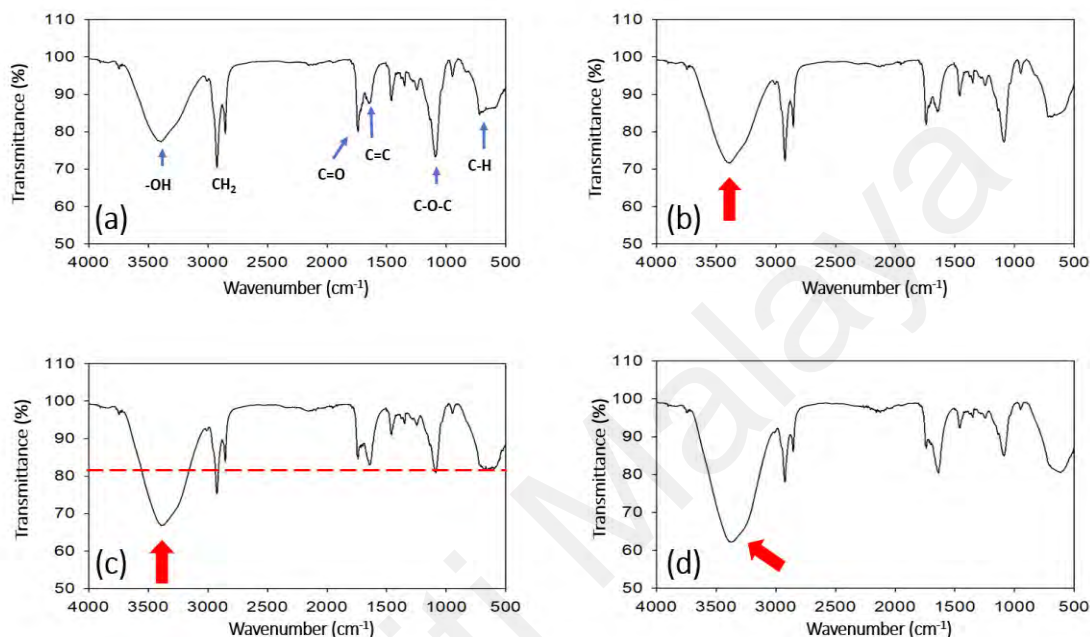

Figure 4.16: The FTIR spectra of ternary-phase system consisting CrEL/GluO (63:37) and sunflower oil at different water content of (a) 20, (b) 30, (c) 40 and (d) 50 % w/w.

4.3.3 Small-angle X-ray scattering (SAXS)

The interpretation of X-ray scattering patterns can support the existence of bi-continuous/lamellar structure at the emulsion inversion point (EIP). Mixed surfactants of CrEL/GluO (63:37) in sunflower oil at fix ratio of 60:40 was studied at different water content starting from 20 to 50 % to detect the existence of lamellar structure. Figure 4.17 shows that a peak (red arrow) starts to appear at $q = 0.03$ Å^{-1} in 40 % water content indicating the surfactants stack together forming a continuous interfacial film of a well-ordered structure. Using the SAXSquant software, it shows that the peak was in

alignment with the lamellar structure (with a thickness of 20.584 nm). At 50% water content, the peak intensity starts to drop indicating the interfacial film of surfactants starts to disperse to form O/W nanoemulsion. This result indicates that the phase inversion point of the system occurred at 40 % water content.
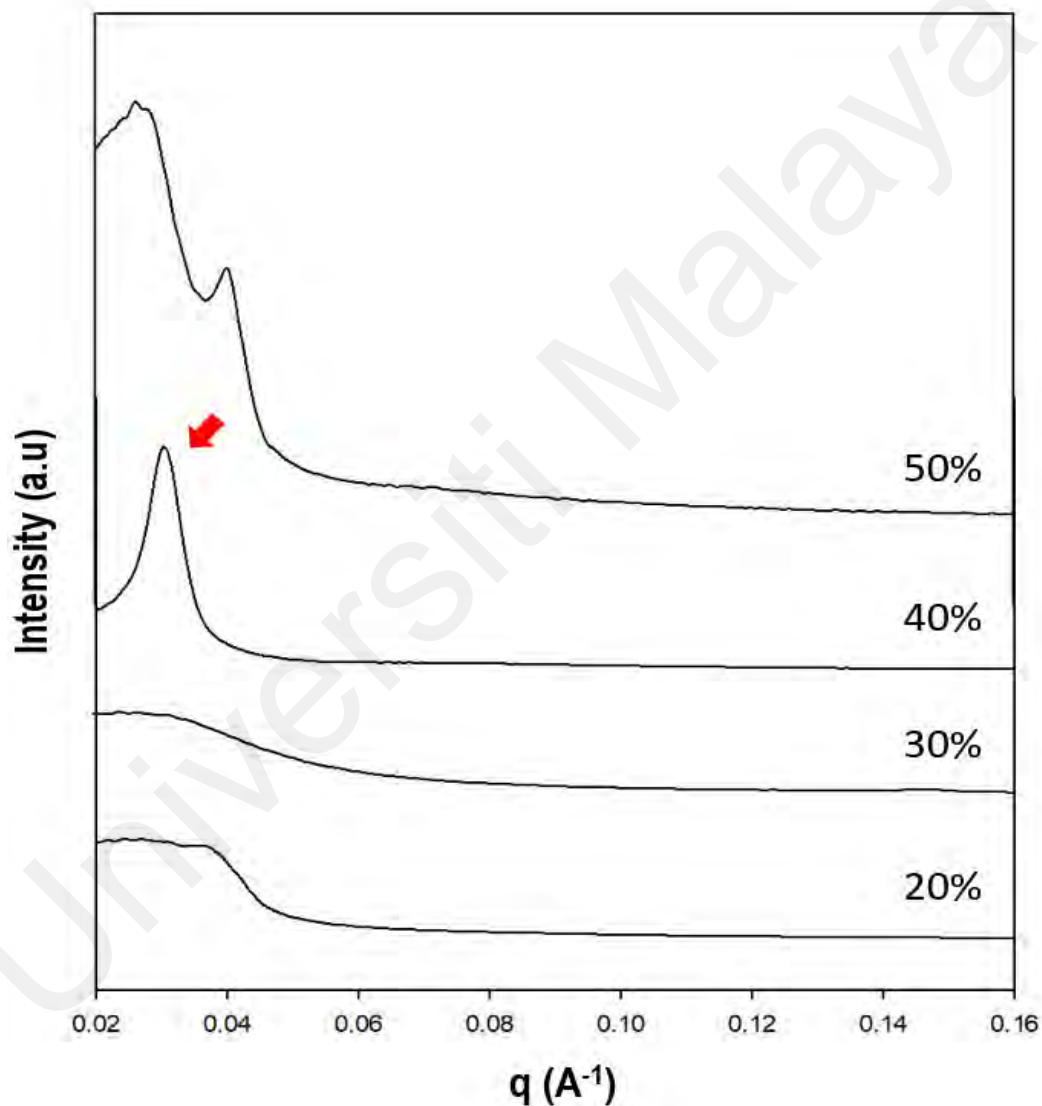
Figure 4.17: Small angle X-Ray (SAX) scattering for a ternary-phase system consisting of CrEL/GluO (63:37) and sunflower oil (60:40) at a different percentage of water content.

64

Figure 4.18 shows the X-ray scattering pattern of CrEL:GluO (63:37) in four types of vegetable oil i.e. sunflower, olive, palm and coconut oil at fix S:O ratio of 60:40. The water content was fixed at 40 %. The presence of a peak at q =0.03 Å^{-1} in the sample containing sunflower and coconut oil indicates the formation of bi-continuous/lamellar structure with the thickness of 20.584 and 26.276 nm, respectively.

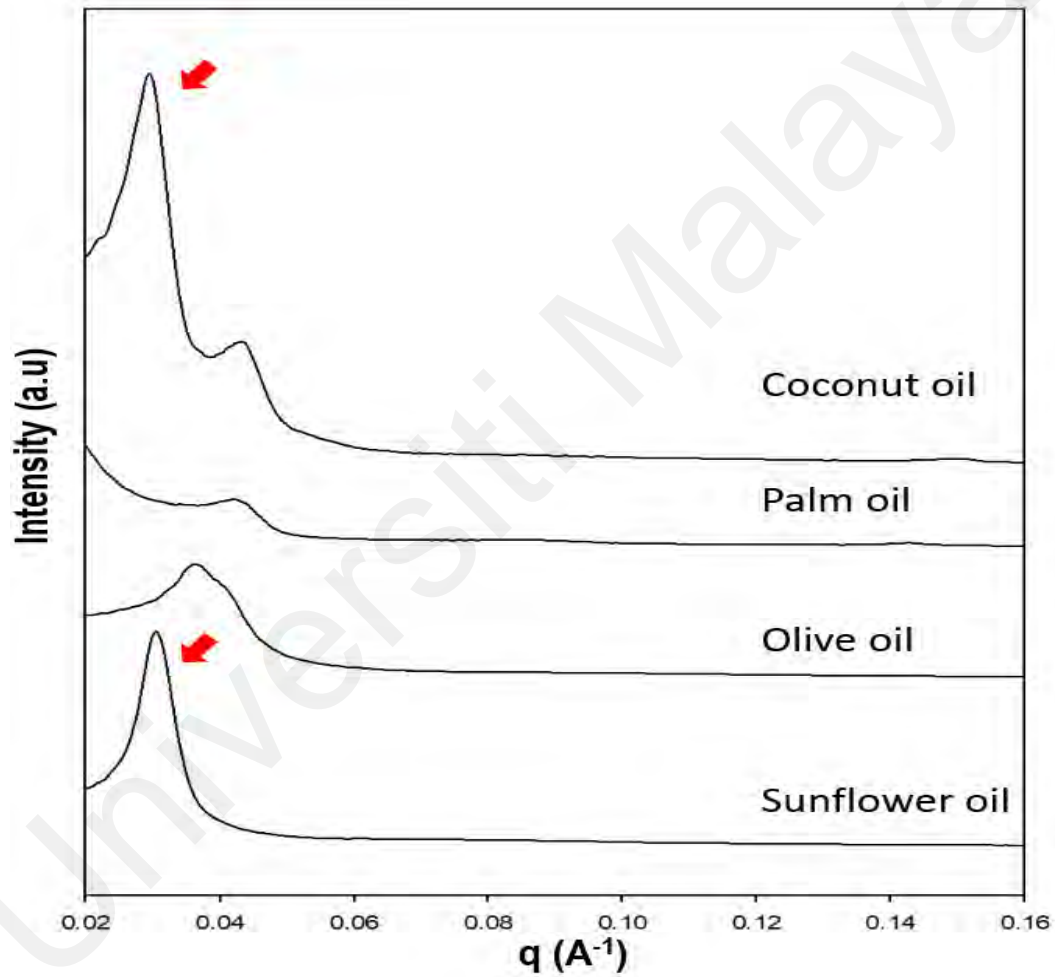**Figure 4.18: The SAX scattering for a ternary-phase system consisting of CrEL/GluO (63:37) and different vegetable oils (60:40) at 40 % of water content.**

4.4 Possible formation of nanoemulsion using surfactant mixture of glucose monooleate and cremophor EL

Nanoemulsion can be obtained using GluO-incorporated surfactant mixture at an optimum formulation. The mechanism that leads to the production of nanoemulsion involves the formation of a bi-continuous/lamellar structure. This is verified through OPM analysis as shown in in Figure 4.13a and 4.13d whereby birefringence appearance was detected. In addition, the presence of lamellar peak in SAXS spectra (Figure 4.18) in ternary system containing sunflower and coconut oil support this hypothesis.

Fourier-transform infrared (FTIR) analysis provides a further understanding of the emulsification process using Tw-80, Sp-80 and GluO-incorporated surfactant mixture. Tw-80 incorporated surfactant mixture shows that the sudden increase of –OH absorbance (3300 cm^{-1}) after 40% water content suggest the phase inversion from W/O to O/W emulsion did not go through the proper formation of the bi-continuous/lamellar structure at EIP. The phase inversion maybe catastrophic which involves the formation of multiple emulsion (O/W/O) at EIP that will result in the production of coarse emulsion with further addition of water (Figure 4.19).

In contrast, Sp-80 and GluO-incorporated surfactant mixture show a different pattern of FTIR spectra. The -OH absorbance (3300 cm^{-1}) shows gradual changes in intensity with the addition of water (Figure 4.15 and 4.16). This provide the idea that the phase inversion involves the proper formation of bi-continuous/lamellar phase that ~~will~~ lead to the formation of nano-sized oil droplets. The emulsification starts with the formation of water droplets in a continuous oil phase (W/O emulsion). Upon addition of water

phase–into the Sp-80- or GluO-incorporated surfactant-oil system, the water droplets coalesced and elongated, which eventually bring to the formation of a bi-continuous/lamellar structure. Beyond this point, the preferred curvature of surfactants layer changes from towards water to towards oil (W/O to O/W emulsion). Therefore, further addition of water will result in the dispersion of the system into smaller size oil droplets hence resulting in the formation of nanoemulsion (Figure 4.19)
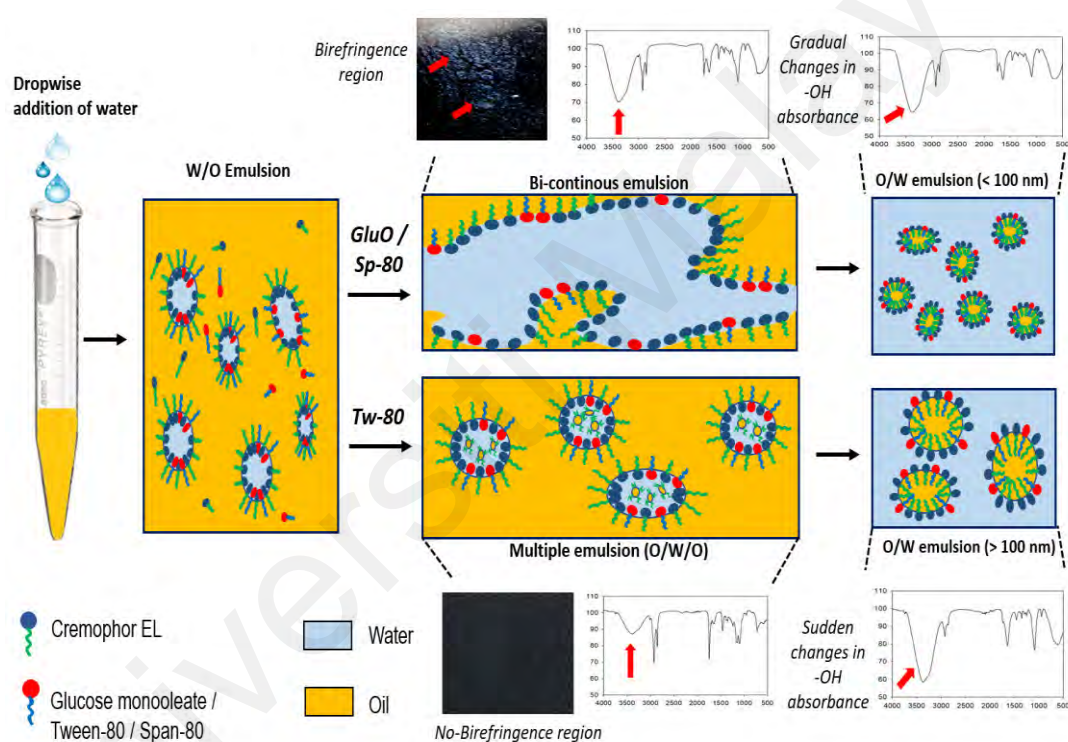

Figure 4.19: Hypothetical mechanism of Tw-80 and Sp-80/GluO-surfactant mixture in the formation of O/W emulsion.

CHAPTER 5: CONCLUSION

In this study, the synthesis of glucose monoleate (GluO) using lipase was successfully conducted and used to produce nanoemulsion through phase inversion composition (PIC), a low energy method. The emulsification ability of GluO was compared with other commercially available non-ionic surfactants that shared the same hydrophobic tail (oleic acid) which are Tween-80 and Span-80. Being a hydrophobic surfactant, the GluO cannot solubilize the oil when used as a single surfactant and thus a coarse emulsion was obtained. However, when used together with cremophor EL (a hydrophilic surfactant) as co-surfactant, O/W nanoemulsion can be obtained. The ratio of CrEL/GluO was fixed at 63:37, based on the previous study. This surfactant mixture was used to emulsify four different types of vegetable oils i.e. sunflower, palm, olive, and coconut oil. From the result, only sunflower and coconut oil can be emulsified into nanoemulsion while palm and olive would only result in a coarse emulsion. This probably due to different lipid composition of each vegetable oils that affect the emulsification process. Glucose monoleate (GluO)-incorporated surfactant mixture able to produce smaller nano-sized oil droplets at higher oil ratio as compared to Tween-80 and Span-80. This shows that glucose monooleate has good potential as a surfactant in the development of nanoencapsulation system. The phase inversion emulsification of vegetable oil (with a surfactant-to-oil ratio of 60:40) using CrEL/GluO surfactant mixture (63:37) was studied using OPM, SAXS and FTIR. From a water penetration study, birefringence region was detected under OPM in samples containing sunflower and coconut oil indicating the formation of bi-continuous/lamellar structure. The SAXS data verified the formation of bi-continuous/lamellar structure and the EIP of the

ternary-phase system was determined at 40% water content. Further investigation of intermolecular interaction among components in the system at different water content was conducted using FTIR. The results suggested that the surfactant molecules aligned themselves in between oil-water phase stream (i.e. formation of bi-continuous/lamellar structure) at 40 % water content. All formulation that were able to show the formation of bi-continuous/lamellar structure during emulsification could produce an emulsion with nano-sized oil droplets. Therefore, it can be concluded that the formation of this structure is necessary to obtain nanoemulsion through PIC technique.

Based on this study, further work is recommended including construction of ternary phase diagram of the emulsion system, determining the HLB and HLD value of GluO/CrEL mixture, stability of the nanoemulsion formation and encapsulation efficiency with lipophilic bioactive compounds. Besides that, the purification method for GluO can be improved by including chromatography technique such as reversed-phase high performance liquid chromatography (RP-HPLC) thus the purity of the yielded GluO can be determined.

REFERENCES

Ahmad, E., Masoud, M., Haji, B. S., Mohammad, A. O., Mustafa, A., & Eid, M. (2012). The influence of sucrose ester surfactants and different storage conditions on the preparation of a novel *Swietenia macrophylla* oil nano-emulsion. *International Research Journal of Pharmacy, 3*(6), 199-207.

Akinola, F., & Oguntibeju, O. (2010). Physico-chemical properties of palm oil from different palm oil local factories. *Journal of Food Agriculture and Environment, 8*(3), 264-269.

Almuhaideb, A., Papathanasiou, N., & Bomanji, J. (2011). 18F-FDG PET/CT imaging in oncology. *Annals of Saudi Medicine*, *31*(1), 3-13.

An, D., & Ye, Z. (2017). Synthesis and surface activity of novel glucose ester surfactants containing carbohydrate and hydrocarbon chain. *Journal of Dispersion Science and Technology*, *38*(8), 1181-1186.

Andhale, R. R., & Kalbhor, T. L. (2018). Fatty acid profile and quality assessment of safflower (Carthamus tinctorius) oil. *Journal of Pharmacognosy and Phytochemistry*, *7*(2), 3581-3585.

Aqilah, N., Channip, A. G. A., Chok, P., Hwa, H., Ja, F., & Anwar, M. Y. (2018). Physicochemical properties , antioxidant capacities , and metal contents of virgin coconut oil produced by wet and dry processes. *Food Science & Nutrition*, *6*, 1298-1306.

Ariffin, M. F. K., Annuar, M. S. M., & Heidelberg, T. (2014). Surfactant synthesis via lipase esterification of methyl α-d-glucopyranoside with selected aliphatic carboxylic acids. *Journal of Surfactants and Detergents*, *17*(4), 683-692.

Arumugam, M., Raman, M., & Eagappan, K. (2014). Cold Pressed virgin coconut oil from full fat coconut flakes a functional oil. *International Journal of Pharmacy and Pharmaceutical Sciences*, *6*(6), 186-190.

Arun, S., Rishikesh, D., Mohite, A., & Hajare, A. A. (2018). Screening of safflower oil microemulsion for enhancing bioavailability of lovastatin. *International Journal of Pharma Sciences and Research, 6*(1), 28-49.

Ashokkumar, C., Murugan, B., Baskaran, D., & Veerapandian, V. (2018). Physicochemical properties of olive oil and its stability at different storage temperatures. *International Journal of Chemical Studies, 6*(2), 1012–1017.

Bhadani, A., Iwabata, K., Sakai, K., Koura, S., Sakai, H., & Abe, M. (2017). Sustainable oleic and stearic acid based biodegradable surfactants. *RSC Advances*, *7*(17), 10433–10442.

Boateng, L., Ansong, R., Owusu, W. B., & Steiner-asiedu, M. (2016). Coconut oil and palm oil ' s role in nutrition , health and national development : A review. *Ghana Medical Journal, 50*(3), 189–196.

Chung, C., & McClements, D. J. (2018). Characterization of physicochemical properties of nanoemulsions: appearance, stability, and rheology. *Nanoemulsions: Formulation, Applications, and Characterization*. Academic Press: Elsevier.

Croy, S. R., & Kwon, G. S. (2005). Polysorbate 80 and cremophor EL micelles deaggregate and solubilize cystatin at the core-corona interface. *Journal of Pharmaceutical Sciences*, *94*(11), 2345–2354.

Devanathan, S., January, R., Nir, T., & Nir, T. (1991). Determination of critical micelle concentration using a near-infrared hydrophobicity of surfactants probe. *Microchemical Journal, 172*(191), 165–172.

Dinarvand, R., & Atyabi, F. (2005). Effect of surfactant HLB and different formulation variables on the properties of poly-D,L-lactide microspheres of naltrexone prepared by double emulsion technique. *Journal of microencapsulation*, *22*(2), 139–151.

Engelbrekt, C., Sørensen, K. H., Zhang, J., Welinder, A. C., Jensen, P. S., & Ulstrup, J. (2009). Green synthesis of gold nanoparticles with starch-glucose and application in bioelectrochemistry. *Journal of Materials Chemistry*, *19*(42), 7839–7847.

Fuenmayor, C. A., & Otoni, C. G. (2018). Nanoemulsions : synthesis, characterization, and application in bio-based active food packaging. *Comprehensive Reviews in Food Science and Food Safety, 18,* 264-285

Gu, L., Faig, A., Abdelhamid, D., & Uhrich, K. (2013). Sugar-based amphiphilic polymers for biomedical applications: From nanocarriers to therapeutics. *Accounts of Chemical Research, 47*(10), 2867-2877.

Gumel, A. M., Annuar, M. S. M., Heidelberg, T., & Chisti, Y. (2011). Lipase mediated synthesis of sugar fatty acid esters. *Process Biochemistry*, *46*(11), 2079–2090.

Gupta, A., Badruddoza, A. Z. M., & Doyle, P. S. (2017). A general route for nanoemulsion synthesis using low-energy methods at constant temperature. *Langmuir*, *33*(28), 7118–7123.

Gupta, A., Eral, H. B., Hatton, T. A., & Doyle, P. S. (2016). Nanoemulsions: Formation, properties and applications. *Soft Matter*, *12*(11), 2826–2841.

Gurpreet, K., & Singh, S. K. (2018). Review of Nanoemulsion Formulation and Characterization Techniques. *Indian Journal of Pharmaceutical Sciences*, *80*(5), 781–789.

Håkansson, A., & Rayner, M. (2018). General Principles of Nanoemulsion Formation by High-Energy Mechanical Methods. *Nanoemulsions: Formulation, Applications, and Characterization*. Academic Press: Elsevier.

Hindi, S. (2016). Birefringence of bio-based liquid crystals. *Biocrystals Journal, 1*(1), 13-25.

Ishak, K. A., Annuar, M. S. M. (2016). Phase inversion of medium-chain-length poly-3-hydroxyalkanoates (mcl-PHA)-incorporated nanoemulsion: effects of mcl-PHA molecular weight and amount on its mechanism. *Colloid and Polymer Science, 294*(12), 1969–1981.

Ishak, K. A., Annuar, M. S. M. (2017). Facile Formation of Medium-Chain-Length Poly-3-Hydroxyalkanoates (mcl-PHA)-Incorporated Nanoparticle Using Combination of Non-Ionic Surfactants. *Journal of Surfactants and Detergents*, *20*(2), 341–353.

Ishak, K. A., Annuar, M. S. M., & Ahmad, N. (2017). Optimization of Water/Oil/Surfactant System for Preparation of Medium-Chain-Length Poly-3-Hydroxyalkanoates (mcl-PHA)-Incorporated Nanoparticles via Nanoemulsion Templating Technique. *Applied Biochemistry and Biotechnology*, *183*(4), 1191–1208.

Ishak, K. A., Zahid, N. I., Velayutham, T. S., Annuar, M. S. M., & Hashim, R. (2019). Effects of lipid packing and intermolecular hydrogen bond on thermotropic phase transition of stearyl glucoside. *Journal of Molecular Liquids*, *281,* 20–28.

Jintapattanakit, A. (2018). Preparation of nanoemulsions by phase inversion temperature (PIT) method. *Pharmaceutical Sciences Asia*, *45*(1), 1–12.

Khoee, S., & Yaghoobian, M. (2017). Chapter 6 - Niosomes: a novel approach in modern drug delivery systems. *Nanostructures for Drug Delivery*. Elsevier.

Klang, V., Schwarz, J. C., Matsko, N., Rezvani, E., El-Hagin, N., Wirth, M., & Valenta, C. (2011). Semi-solid sucrose stearate-based emulsions as dermal drug delivery systems. *Pharmaceutics*, *3*(2), 275-306.

Komaiko, J. S., & Mcclements, D. J. (2016). Formation of food-grade nanoemulsions using low-energy preparation methods: A review of available methods. *Comprehensive Reviews in Food Science and Food Safety*, *15*(2), 331-352.

Kulkarni, C. V., Wachter, W., Iglesias-Salto, G., Engelskirchen, S., & Ahualli, S. (2011). Monoolein: A magic lipid? *Physical Chemistry Chemical Physics*, *13*(8), 3004-3021.

Li, H., Dang, L., Yang, S., Li, J., & Wei, H. (2016). The study of phase behavior and rheological properties of lyotropic liquid crystals in the LAS / AES / H 2 O system. *Colloids and Surfaces A: Physicochemical and Engineering Aspects*, *495,* 221-228.

Lv, G., Wang, F., Cai, W., & Zhang, X. (2014). Characterization of the emulsions formed by catastrophic phase inversion. *Colloids and Surfaces A: Physicochemical and Engineering Aspects*, *450,* 141-147.

Mahdi, E. S., Sakeena, M. H., Abdulkarim, M. F., Abdullah, G. Z., Sattar, M. A., & Noor, A. M. (2011). Effect of surfactant and surfactant blends on pseudoternary phase diagram behavior of newly synthesized palm kernel oil esters. *Drug Design, Development and Therapy*, *5,* 311-323.

Mancini, A., Imperlini, E., Nigro, E., Montagnese, C., Daniele, A., Orrù, S., & Buono, P. (2015). Biological and Nutritional Properties of Palm Oil and Palmitic Acid: Effects on Health. *Molecules, 20,* 17339–17361.

Mańko, D., & Zdziennicka, A. (2015). Sugar-based surfactants as alternative to synthetic ones. *Annales UMCS, Chemia*, *70*(1), 161-168.

Maratou, E., Dimitriadis, G., Kollias, A., Boutati, E., Lambadiari, V., Mitrou, P., & Raptis, S. A. (2007). Glucose transporter expression on the plasma membrane of resting and activated white blood cells. *European Journal of Clinical Investigation*, *37*(4), 282–290.

McClements, D. J., & Jafari, S. M. (2018). General Aspects of Nanoemulsions and Their Formulation. *Nanoemulsions: Formulation, Applications, and Characterization*. Academic Press: Elsevier.

Mcclements, D. J., Rao, J., Mcclements, D. J., & Rao, J. (2017). Food-grade nanoemulsions: formulation, fabrication, properties, performance, biological fate, and potential toxicity: Critical reviews. *Food Science and Nutrition, 51*(4), 285-330.

Mehta, S. K., Kaur, G., & Bhasin, K. K. (2010). Tween-embedded microemulsions-Physicochemical and spectroscopic analysis for antitubercular drugs. *American Association of Pharmaceutical Scientists, 11*(1), 143-153.

Navale, A. M., & Paranjape, A. N. (2016). Glucose transporters: physiological and pathological roles. *Biophysical Reviews*, *8*(1), 5-9.

Perazzo, A., Preziosi, V., & Guido, S. (2015). Phase inversion emulsification: Current understanding and applications. *Advances in Colloid and Interface Science*, *222,* 581-599.

Ren, K., & Lamsal, B. P. (2017). Synthesis of some glucose-fatty acid esters by lipase from *Candida antarctica* and their emulsion functions. *Food Chemistry*, *214*, 556-563.

Rodrigues, F. V. S., Diniz, L. S., Sousa, R. M. G., Honorato, T. D., Simão, D. O., Araújo, C. R. M., Siqueira-Moura, M. P. (2018). Preparation and characterization of nanoemulsion containing a natural naphthoquinone. *Quimica Nova*, *41*(7), 756-761.

Roger, K. (2016). Nanoemulsification in the vicinity of phase inversion: Disruption of bicontinuous structures in oil/surfactant/water systems. *Current Opinion in Colloid and Interface Science*, *25*, 120-128.

Singh, Y., Meher, J. G., Raval, K., Khan, F. A., Chaurasia, M., Jain, N. K., & Chourasia, M. K. (2017). Nanoemulsion: Concepts, development and applications in drug delivery. *Journal of Controlled Release*, *252*, 28-49.

Tyler, A. I. I., Law, R. V, & Seddon, J. M. (2015). X-ray diffraction of lipid model membranes. *Methods in Molecular Biology, 1232*, 199-225.

Wędrowski, M., Waśniowski, P., Wędrowska, E., Piskorska, E., Czuczejko, J., Małkowski, B., & Zukow, W. (2018). Synthesis and application of (18F) fluorodeoxyglucose in oncology diagnosis. *Journal of Education, Health and Sport, 7*(12), 481-500.

Zeng, L., Xin, X., & Zhang, Y. (2017). Development and characterization of promising cremophor EL-stabilized O/W nanoemulsions containing short-chain alcohols as a cosurfactant. *RSC Advances*, *7*(32), 19815–19827.

Zhang, X., Sun, X., Li, J., Zhang, X., Gong, T., & Zhang, Z. (2011). Lipid nanoemulsions loaded with doxorubicin-oleic acid ionic complex: Characterization, *in vitro* and *in vivo* studies. *Pharmazie*, *66*(7), 496-505.

Zhang, Z., & McClements, D. J. (2018). Overview of Nanoemulsion Properties: Stability, Rheology, and Appearance. *Nanoemulsions: Formulation, Applications, and Characterization*. Academic Press: Elsevier.

Zhao, K. H., Cai, Y. Z., Lin, X. S., Xiong, J., Halling, P. J., & Yang, Z. (2016). Enzymatic synthesis of glucose-based fatty acid esters in bisolvent systems containing ionic liquids or deep eutectic solvents. *Molecules*, *21*(10), 1-13.

Zheng, Y., Zheng, M., Ma, Z., Xin, B., Guo, R., & Xu, X. (2015). Sugar Fatty Acid Esters. *Polar Lipids: Biology, Chemistry, and Technology*. Elsevier.

LIST OF PUBLICATIONS AND PAPERS PRESENTED

List of Publication.

1. Ishak, K.A., **Fadzil, M.F.A**., & Annuar, M.S.M (2021) Phase Inversion Emulsification of Different Vegetable Oils Using Surfactant Mixture of Cremophor EL and Lipase-Synthesized Glucose Monooleate. *LWT Food Science and Technology, 138*(144), 110568